2018

A Preliminary Study of Smithport Plain Bottle Morphology in the Southern Caddo Area

Robert Z. Selden Jr.
Center for Regional Heritage Research, Stephen F. Austin State University, zselden@sfasu.edu

Bulletin of the TEXAS ARCHEOLOGICAL SOCIETY Volume 89/2018

Britt Bousman and Sarah Morris, Editors

Published by

TEXAS ARCHEOLOGICAL SOCIETY

2018

A Preliminary Study of Smithport Plain Bottle Morphology in the Southern Caddo Area

Robert Z. Selden, Jr.

This study expands upon a previous analysis of the Clarence H. Webb collection, which resulted in the identification of two discrete shapes used in the manufacture of the base and body of Smithport Plain bottles. The sample includes the Smithport Plain bottles from the Webb collection, and four new bottles: two previously repatriated specimens in the Pohler Collection, and two from the Mitchell site (41BW4) to test whether those specimens align morphologically with the Belcher Mound or Smithport Landing specimens. Results indicate significant allometry and a significant difference in Smithport Plain body and base shapes for bottles produced at the Smithport Landing and Belcher Mound sites in northwest Louisiana. The Pohler and Mitchell specimens do not differ significantly from those found at Smithport Landing or Belcher Mound. Analysis of the aggregated sample indicates some significant relationships between bottle shape and size, bottle shape and type, and bottle shape and site, highlighting assemblage-level and type-specific variability. The test of morphological disparity by period indicates a gradual trend toward standardization, and the test of morphological integration indicates that Caddo bottles are significantly integrated, meaning that those discrete traits used to characterize their shape (rim, neck, body, and base) vary in a coordinated manner. The iterative development of this research design can lead to substantive theoretical gains that augment discussions of decorative components and motifs as well as ceramic technological attributes.

Defined as "a vessel with a spheroid or oval body, surmounted by a slender, cylindrical neck," Caddo bottles were initially seen as a somewhat homogenous ceramic form (Harrington 1920:187); some with shapes and motifs so similar to be deemed the work of a single maker (Harrington 1920:188). In a more recent study, Caddo bottles were found to be more symmetrical than bowls and ollas (Selden, Jr. 2017); however, additional work is needed to identify whether—and to what extent—this holds true across a broader range of vessel shapes and types. Caddo vessel shapes are variable among groups and through time, reflecting stylistic, functional, and social change (Perttula 2010). Caddo potters elevated local ceramic production to high art, and "had no superiors short of the Pueblo country" (Swanton 1942:239), leading some analysts to posit that Caddo bottles rest at the apex of Native American ceramic technology (Gadus 2013). A division of the Caddo bottle category has been proposed for northeast Texas that segregates bottle forms into 27 shapes, each with distinct temporal and spatial distributions (Perttula 2015:Figure 2), and novel deployments of geographic information systems are aiding in the refinement of their probable geographic extents (McKinnon 2011).

This effort capitalizes on the quiddity of Caddo bottle shape for a small sample (n = 8) of Smithport Plain bottles previously posited to exhibit morphological differences (Selden Jr. 2018a; Suhm and Jelks 1962; Webb 1959). Three-dimensional (3D) meshes for the Webb Collection and four new samples from one site and one collection were used to test whether a significant difference in shape exists for Smithport Plain bottles by site, followed by a test for allometry. The Smithport Plain bottles were subsequently examined as part of the aggregated sample of Caddo bottles to demonstrate morphological variability, allometry, morphological disparity, and morphological integration among the types (Table 1 and Figure 1).

Taxonomic definitions for Caddo ceramics integrate semiotic and morphological attributes, and each type is characterized by a broad range of vessel shapes that often include bottles, bowls, carinated bowls, ollas, as well as other shapes (Suhm and Jelks 1962; Suhm et al. 1954). The Smithport Plain type was defined by Webb (1959) at the Smithport Landing site (16DS4) in northwest Louisiana and is believed to range in age from the Formative to Early Caddo periods (ca. AD 800–1200) (Webb 1963). All Caddo bottles used in this analysis fall

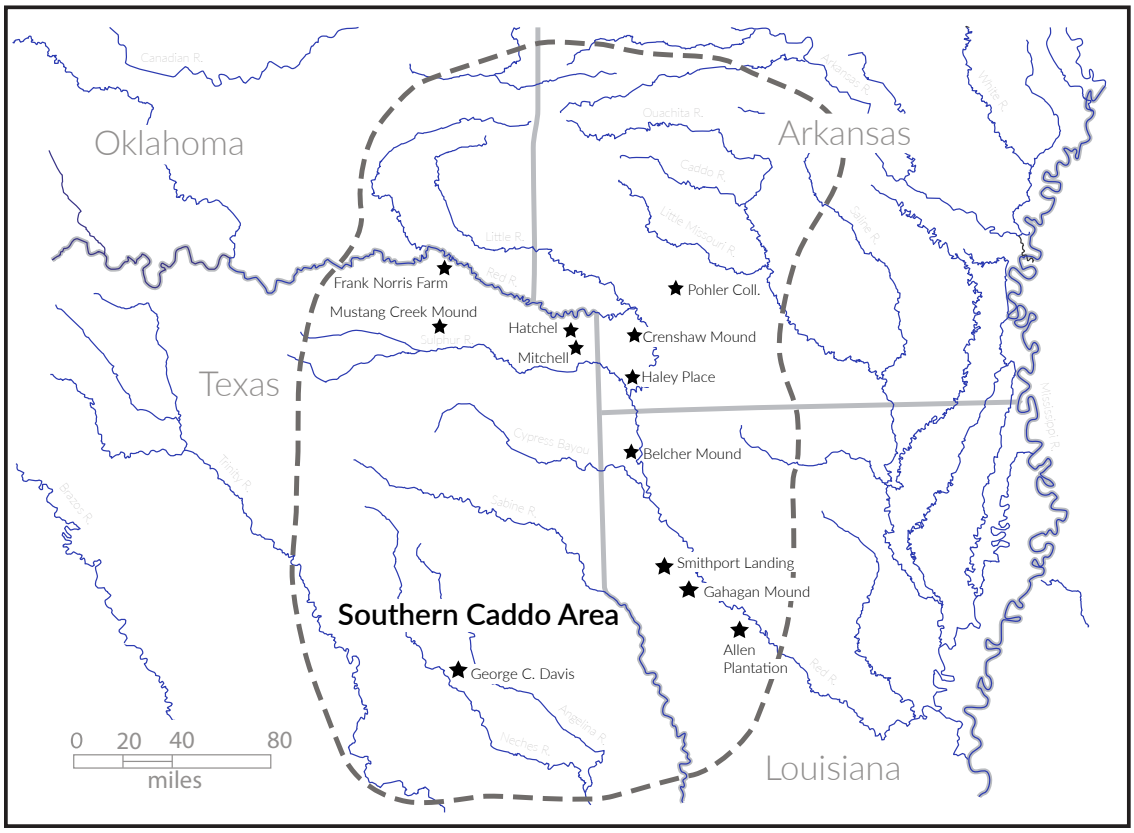

Figure 1. Locations of Allen Plantation, Hatchel, Belcher Mound, Crenshaw Mound, Frank Norris Farm, Gahagan Mound, George C. Davis, Haley Place, Mustang Creek Mound (also known as T. N. Cole), Paul Mitchell (Mitchell), specimens from the Pohler Collection (Clark County, Arkansas), and Smithport Landing.

Table 1. Caddo bottles used in this analysis.

Specimen	Site Name	Trinomial	Context	Museum	Type
256	Belcher Mound	16CD13	Burial 5	LSUMNH	Taylor Engraved
267	Belcher Mound	16CD13	Burial 5	LSEM	Belcher Engraved
269	Belcher Mound	16CD13	Burial 5	NSU	Belcher Engraved
271	Belcher Mound	16CD13	Burial 5	LSUMNH	Taylor Engraved
361	Belcher Mound	16CD13	Burial 9	NSU	Belcher Engraved
363	Belcher Mound	16CD13	Burial 10	NSU	Belcher Engraved
404	Belcher Mound	16CD13	Burial 11	NSU	Hickory Engraved
405	Belcher Mound	16CD13	Burial 11	NSU	Smithport Plain
430	Belcher Mound	16CD13	Burial 12	NSU	Smithport Plain
775	Belcher Mound	16CD13	Burial 15	NSU	Belcher Engraved
784	Belcher Mound	16CD13	Burial 15	LSUMNH	Keno Trailed
787	Belcher Mound	16CD13	Burial 15	LSUMNH	Taylor Engraved
788	Belcher Mound	16CD13	Burial 15	NSU	Belcher Engraved
803	Belcher Mound	16CD13	Burial 15	LSUMNH	Belcher Engraved
805	Belcher Mound	16CD13	Burial 15	NSU	Belcher Engraved
845	Belcher Mound	16CD13	Burial 17	NSU	Belcher Engraved
852	Belcher Mound	16CD13	Burial 17	NSU	Keno Trailed
897	Belcher Mound	16CD13	House 6	NSU	Belcher Engraved
997	Belcher Mound	16CD13	Burial 24	NSU	Belcher Engraved
1054	Belcher Mound	16CD13	Burial 26	LSEM	Taylor Engraved

Table 1. Caddo bottles used in this analysis. *(Continued)*

Specimen	Site Name	Trinomial	Context	Museum	Type
1073	Belcher Mound	16CD13	House 6	NSU	Belcher Engraved
95	Smithport Landing	16DS4	Burial 1	NSU	Smithport Plain
96	Smithport Landing	16DS4	Burial 1	NSU	Hickory Engraved
152	Smithport Landing	16DS4	Burial 10	NSU	Smithport Plain
No #	Smithport Landing	16DS4	Unknown	NSU	Hickory Engraved
142	Allen Plantation	16NA6	Unknown	NSU	Hickory Engraved
955	Gahagan Mound	16RR1	Mound A	NSU	Hickory Engraved
956	Gahagan Mound	16RR1	Mound A	LSUMNH	Hickory Engraved
HFE1	Haley Place	3MI1	Unknown	LSEM	Hickory Engraved
HFE2	Haley Place	3MI1	Unknown	LSEM	Hickory Engraved
HFE3	Haley Place	3MI1	Unknown	LSEM	Hickory Engraved
HFE4	Haley Place	3MI1	Unknown	LSEM	Hickory Engraved
HFE5	Haley Place	3MI1	Unknown	LSEM	Hickory Engraved
55-1-8*	Crenshaw Mound	3MI6	Unknown	CNO	Hickory Engraved
2002-01-18*	Unknown (Clark County, AR)	Pohler Coll	Unknown	CNO	Smithport Plain
2002-01-20*	Unknown (Clark County, AR)	Pohler Coll	Unknown	CNO	Hickory Engraved
2002-01-23*	Unknown (Clark County, AR)	Pohler Coll	Unknown	CNO	Hickory Engraved
2002-01-27*	Unknown (Clark County, AR)	Pohler Coll	Unknown	CNO	Smithport Plain
FS7	Hatchel	41BW3	Unknown	TARL	Hickory Engraved
6-2-67	Paul Mitchell	41BW4		TARL	Smithport Plain
6-2-78	Paul Mitchell	41BW4		TARL	Smithport Plain
6-2-132	Paul Mitchell	41BW4	Unknown	TARL	Hickory Engraved
341-427	Paul Mitchell	41BW4	Burial 9	TARL	Hickory Engraved
341-464	Paul Mitchell	41BW4	Burial 21	TARL	Hickory Engraved
2015-1	George C. Davis	41CE19	Burial F-154	TARL	Hickory Engraved
7	Frank Norris Farm	41RR2	Unknown	TARL	Hickory Engraved
2	Mustang Creek Mound	41RR3	H. O. #568	TARL	Hickory Engraved

The bottle without a number (Webb Collection) is assumed to have come from the Smithport Landing site in fragments. The bottle was later reassembled, but a number was never assigned. * = repatriated to the Caddo Nation of Oklahoma. NSU = Northwestern State University (Williamson Museum); LSUMNS = Louisiana State University Museum of Natural Science; CNO = Caddo Nation of Oklahoma; TARL = Texas Archeological Research Laboratory; LSEM = Louisiana State Exhibit Museum.

under the Native American Graves Protection and Repatriation Act (NAGPRA), excepting those found in House 6 at the Belcher Mound site (see Table 1). The Caddo Nation of Oklahoma granted permission to scan the collections with the provision that any scan data used in the analysis must not include the texture (color) file. Full-resolution scan data were forwarded to the Caddo Nation of Oklahoma with the texture applied. This provides them with an accurate 3D record of each vessel, and a means of viewing a collection of bottles that is curated across numerous repositories.

Geometric Morphometrics in Archeology

Analyses of artifact shape are neither new or novel (Okumura and Araujo 2018), and it is not surprising that geometric morphometrics (GM) (sensu Corti (1993)) has captivated analysts of material culture due to the substantive contribution of morphology to lithic (Fox 2015; Thulman 2012; Wilczek et al. 2015) and ceramic typologies (Girrulat 2006; Topi et al. 2017; Wilczek et al. 2014), additional categories of material culture (Chitwood 2014; Ros et al. 2014; Windhager et al. 2012), and

novel applications (Barceló 2010; Lenardi and Merwin 2010). The earliest study of artifacts was an analysis of irregular shapes by elliptic Fourier analysis (EFA) (Gero and Mazzullo 1984), and the adoption of the method by the archaeological community has grown to include an impressive array of applications (Figure 2).

EFA has been employed at an increasing rate in lithic and ceramic analyses (Cardillo et al. 2010; Costa 2010; Fox 2015; Ioviţă 2009, 2010, 2011; Ioviţă and McPherron 2011; Smith et al. 2014; Wilczek et al. 2014), where new approaches advance archeological applications. Creative research designs are also being developed to address challenges with incomplete specimens in the archeological record (Byrne et al. 2016; Rezek et al. 2011; Smith 2010; Smith and DeWitt 2016; Smith and Goebel 2018). These advancements have aided in the development of a useful suite of protocols applicable to wide-ranging research questions.

The recent fluorescence of landmark-based applications has been driven by advances in anthropology (Bookstein et al. 2004; Elewa 2010; Richtsmeier et al. 1992; Slice 2007) and a variety of other research domains (Adams et al. 2004, 2013; Bookstein 1982, 1991, 2016; Jensen 2003; MacLeod 2017; Marcus et al. 1996; Rohlf 1990, 1999; Rohlf and Marcus 1993; Rohlf and Slice 1990; Zelditch et al. 2004) that articulate with the rise of the Procrustes paradigm (Adams et al. 2013:8). Archaeological applications have included two-dimensional (2D) analyses of Clovis technology in North America (Buchanan and Collard 2010; Buchanan et al. 2011; Buchanan et al. 2015; Buchanan et al. 2013; Eren et al. 2015), Fishtail or Fell projectile points in South America (Castiñeira et al. 2011; Loponte et al. 2015), bifacial points from the Umbu Tradition in Brazil (Okumura and Araujo 2013, 2014, 2017), lanceolate points—*ayampitin*—from Argentina (Rivero and Heider 2017), the size and shape of projectile points from southern Patagonia (Charlin et al. 2014; Charlin and González-José 2012), bifacial tools from southern Poland (Serwatka 2015), Final Palaeolithic large tanged points (Serwatka and Riede 2016), Paleoindian point types from Florida (Thulman 2012) and the Southern High Plains (Buchanan et al. 2007), ceramics from Casas Grandes (Topi et al. 2017), flake morphology (Picin et al. 2014), and reduction effects (de Azevedo et al. 2014). All of these studies capitalize on the morphological variation that occurs in a single plane (Buchanan and Collard 2010; Velhagen and Roth 1997).

For research designs that incorporate questions associated with more complex geometry, 3D landmark-based approaches may be more appropriate. Examples from the literature include the development of novel tools and applications (Lycett et al. 2006) that cover a broad range of artifact categories including projectile points (Shott 2011; Shott and Trail 2010), bifaces (Archer and Braun 2010; Archer et al. 2015; Archer et al. 2016), percussive tools (Caruana et al. 2014), flake scars (Sholts et al. 2012), flake tools (Archer et al. 2017), handaxes (Lycett 2009; Lycett et al. 2010; Lycett and von Cramon-Taubadel 2013; Lycett et al. 2016; Wang et al. 2012), and Caddo ceramics (Selden Jr. 2017, 2018a; Selden Jr. et al. 2014). This study adduces the variation that occurs within a single plane (widest vessel profile) for a sample of Caddo bottles; however, 3D data were required to identify the widest profile. Additionally, a variety of landmark and semilandmark configurations are in development that provide for a more robust analysis of 3D morphology associated with specific elements of vessel morphology.

Methods

Bottles were scanned with a Creaform GoSCAN 50 at a 0.8 mm resolution or a Creaform GoSCAN20 at 0.5 mm resolution depending on their size. Scanner calibration was optimized prior to each scan, with positioning targets required for increased accuracy. Shutter speed was reconfigured in each instance; clipping planes were established to reduce the amount of superfluous data collected during each scan. Following data collection, resolution for the GoSCAN 50 meshes was increased to 0.5 mm, and meshes from both scanners were transferred to VXmodel where the final mesh was rendered following application of the *clean mesh* function. This was used to remove isolated patches, self-intersections, spikes, small holes, singular vertices, creased edges, narrow triangles, outcropping triangles, narrow bridges, and non-manifold triangles prior to export as an ASCII stl file. The stl functions as a backup, and the ply was subsequently imported to Geomagic Design X (Dx).

Prior to pursuing the mixed-method analysis employing data from two different scanners, two meshes of the same object—produced with the Creaform GoSCAN 50 and GoSCAN 20—were imported to a computer-aided inspection program (Geomagic Control X) in an effort to identify any

significant deviations that may exist between the meshes prior to the GM analysis (Figure 2). The tolerance level for the inspection was selected using the highest resolution of the GoSCAN 20 (0.1 mm). Small areas of the rim exhibited minor differences while the remainder of the vessel was at or below the arbitrary 0.1 mm tolerance; thus, results fell within an acceptable error range.

The histogram shown in Figure 2 illustrates the Gaussian distribution for the number of errors over the whole deviation. The graph is split into six segments: 1-Sigma at 31 percent from the average to the maximum deviation in each direction, 2-Sigma at 69 percent from the average to the maximum deviation in each direction, and 3-Sigma at 93.3 percent from the average to the maximum deviation in each direction. The average (AVG) is the sum of all deviations divided by the number of all deviations, and the RMS is the square root of all squared deviations divided by the number of all deviations (sometimes referred to as the effective deviation). In tolerance (In Tol) and out tolerance (Out Tol) percentages indicate the percentage of deviations in or out of a given tolerance, and over tolerance (Over Tol) and under tolerance (Under Tol) percentages indicate the percentage of deviations over (positive direction) or under (negative direction) the tolerance range by the mesh normal of the reference mesh.

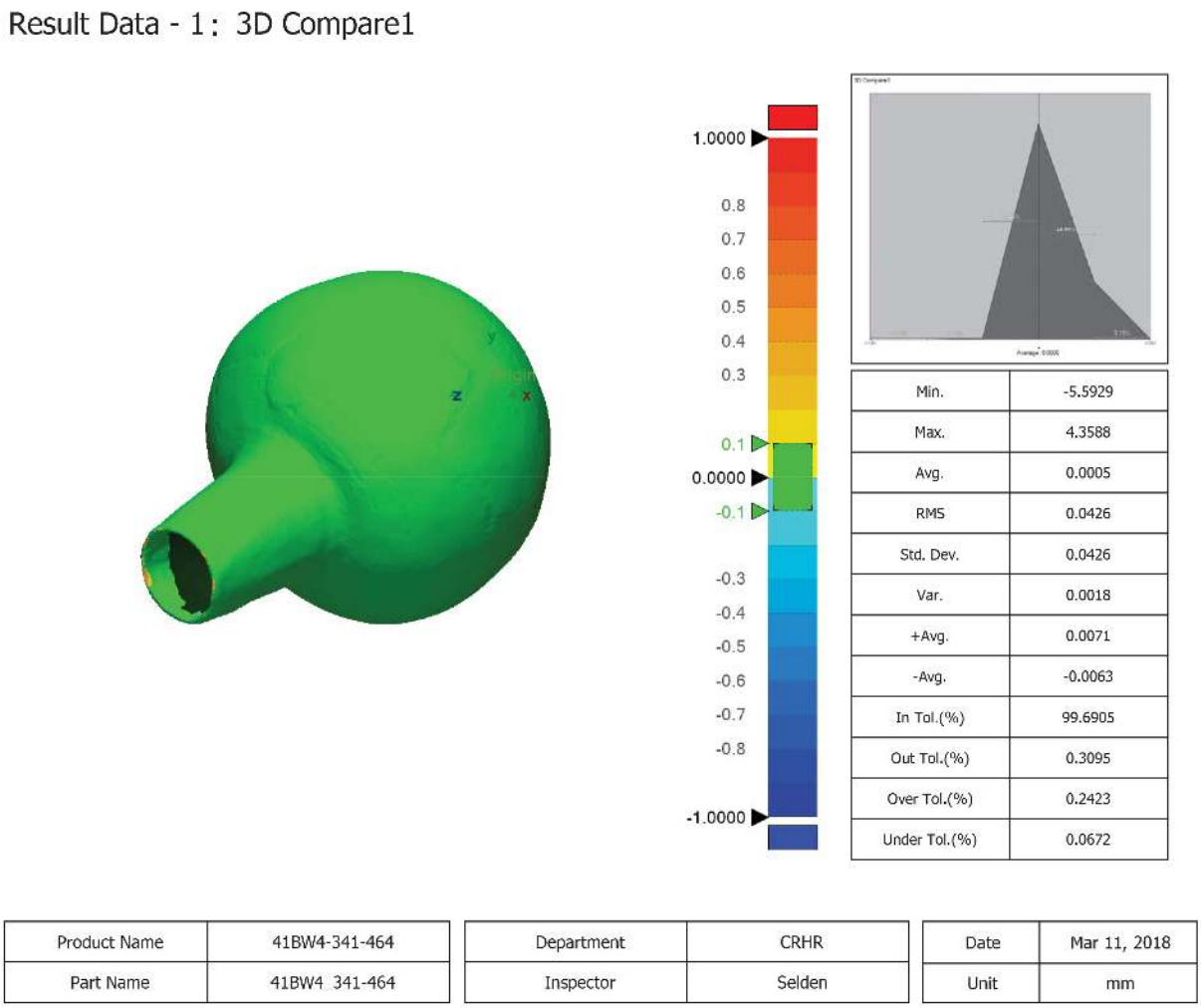

Min.	-5.5929
Max.	4.3588
Avg.	0.0005
RMS	0.0426
Std. Dev.	0.0426
Var.	0.0018
+Avg.	0.0071
-Avg.	-0.0063
In Tol.(%)	99.6905
Out Tol.(%)	0.3095
Over Tol.(%)	0.2423
Under Tol.(%)	0.0672

Product Name	41BW4-341-464	Department	CRHR	Date	Mar 11, 2018
Part Name	41BW4 341-464	Inspector	Selden	Unit	mm

Figure 2. Results of 3D compare for the GoSCAN 50 and GoSCAN 20 meshes of bottle 41BW4 341-464 indicating that 99.6905 percent of the vessel falls within the arbitrary 0.1 mm tolerance.

Alignment and Reference Geometry

Following transfer to Dx, each mesh was subjected to an additional quality check to eliminate non-manifold poly-vertices, folded poly-faces, dangling poly-faces, small clusters, small poly-faces, non-manifold poly-faces, crossing poly-faces, and small tunnels. Due to the paucity of homologous landmarks on cultural artifacts (Lycett 2009), reference geometry was constructed around each vessel in a manner that yielded a replicable configuration of nine landmarks, and 46 equidistant semilandmarks along the widest vessel profile, with notable similarities to previous landmark configurations used by Girrulat (2006:Figure 4), Selden Jr. et al. (2014:Figure 5), Selden, Jr. (2018a:Figure 3), and Topi et al. (2017:Figure 4), all of which largely follow Birkhoff (1933).

The first component of reference geometry added, and the principal assumption, was a reference vector. A sampling ratio of 100 percent was used to apply the reference vector on a revolving axis, after which a reference point was added by projecting it atop the mesh surface at the location where the reference vector exits the base of the vessel. A reference plane was inserted using the *pick multiple points* function, by adding a series of 10 points around the circumference of the bottle's base. Each element of reference geometry (vector, point, and plane) was then used in an interactive 3-2-1 alignment where the vessel was aligned to a global origin, orienting it in 3D space where it sat upright atop a planar surface (assumed to be the intent of the maker). Following alignment, the reference plane and point were deleted.

The widest profile is defined as the location on a mesh that lies farthest from that point where the reference vector exits the vessel base while oriented atop the planar surface. To identify that location, a mesh sketch was generated with the planar method using the plane at the base of the vessel to identify and sketch the widest vessel circumference. By using the plane located at the base of the vessel for the sketch, the point at which the reference vector exits the mesh remains linked to the remainder of the reference geometry. A circle was then sketched using the vector as the center, extending outward until the whole of the vessel fit within. Using the mesh sketch, a cylinder (surface) was extruded around the vessel. The accuracy analyzer in Dx was then used to identify the point on the vessel with the lowest deviation from the extruded surface, and a plane (MPlane) was inserted coplanar to the vector and oriented to the widest point, bisecting the vessel along the widest profile.

Using the MPlane as the basis for a second mesh sketch, a spline with 15 interpolation points was sketched on one rim. Above that sketch, a horizontal line was added where both the spline and horizontal line determine the horizontal tangent of the rim. A vertical line was subsequently added that bisected the rim at the location of the tangent. This operation was repeated for the opposing rim. The addition of this added step was necessary because surface scanners are unable to collect data from the interior of the bottles, so the spline needed to be cut in a replicable location. Since the Smithport Plain bottles exhibit slightly inverted-to-vertical rims, the preceding step was extended to include an additional measure. A line was drawn between each rim tangent, then a second from the intersection of the line and reference vector to a point 10 mm down the vector, where a horizontal line (parallel with the rim peaks) was inserted to intersect with both external walls of the bottle (Selden, Jr. 2018a:Figure 3). It is at this intersection that the final mesh sketch was cut to discriminate between the neck and rim. While this step admittedly appears odd in the context of a comparison of bottle shapes that all exhibit direct rims, it is of considerable import for inter-type comparisons where other bottle types exhibit differing rim morphologies (i.e., everted, etc.) (Selden, Jr. 2018b).

Using the MPlane as the basis for a third sketch, a spline was populated for the entirety of the silhouetted profile. That spline was split at the location of the horizontal tangent on each rim, and the remaining sections that continued into the bottle interior were deleted. The second split was added at the intersection of the spline and reference vector (center of base). Four additional splits were subsequently added at the juncture of the base/body and body/neck on each side of the vessel at the points of highest curvature. The point of highest curvature used to split the spline was identified using the *curvature* function in Dx, and does not represent an arbitrary location.

Landmarks and Semilandmarks

A total of nine landmarks and 46 semilandmarks segregated each bottle into four discrete components corresponding with the rim, neck, body, and base (Table 2 and Figure 3). Landmarks and semilandmarks were populated along the spline, and

numbering always began on that side of the profile determined to include the widest point. Divisions between each component articulate with those of the spline splits, where landmarks were placed at each point in Table 2, with a series of equidistant semilandmarks between them.

While sliding semilandmarks were an early consideration of this research design, the decision to use equidistant semilandmarks rather than sliding semilandmarks was based upon results from an earlier iteration of the Webb collection analysis (Selden, Jr. 2018a:Figure 3). In the study of the Webb collection, the first landmark and sliding semilandmark configuration did not split the spline between the neck and rim, and when mean shapes were generated for each type, an anomaly, from the everted rims of Belcher Engraved bottles in that case, was added to the otherwise direct or tapered necks of the Hickory

Table 2. Landmarks used in this analysis.

Landmark	Location	Definition
Point01	Rim peak	Horizontal tangent of rim curvature on widest side of vessel
Point06	Rim/Neck	Point of highest curvature (everted rim) or intersection of horizontal line 10 mm below rim tangents (direct rim)
Point15	Neck/Body	Point of highest curvature
Point24	Body/Base	Point of highest curvature
Point28	CenterBase	Intersection of vector and external surface of the 3D mesh
Point32	Body/Base	Point of highest curvature
Point41	Neck/Body	Point of highest curvature
Point50	Rim/Neck	Point of highest curvature (everted rim) or intersection of horizontal line 10 mm below rim tangents (direct rim)
Point55	Rim peak	Horizontal tangent of rim curvature

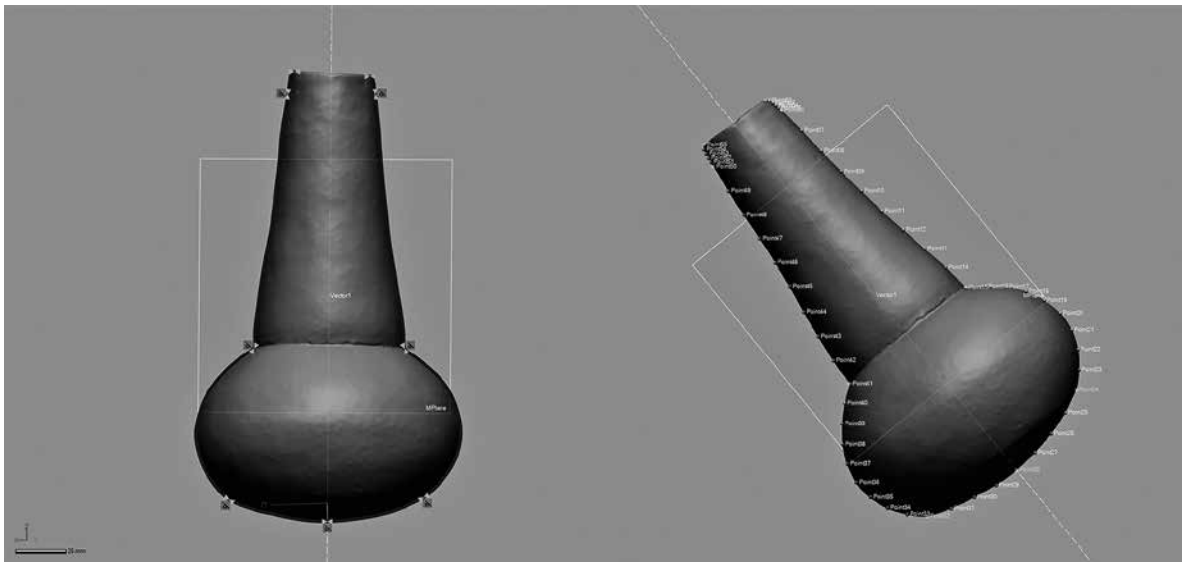

Figure 3. Spline splits for discrete components (rim, neck, body, and base) used in the GM analysis (left) segregated by landmarks (blue), with equidistant semilandmarks (white) populated between (right).

Engraved and Smithport Plain bottles. Given that the use of sliding semilandmarks could potentially influence the results of this analysis by introducing a morphological attribute to specimens where one does not exist, they were abandoned.

Analysis

Landmarks and equidistant semilandmarks were exported as x, y, and z coordinate data from Dx. Those data were aligned to a global coordinate system (Kendall 1981, 1984; Slice 2001), achieved through generalized Procrustes superimposition (Rohlf and Slice 1990) performed in R 3.5.0 (R Development Core Team 2018) using the *geomorph* library v.3.0.6 (Adams et al. 2017; Adams and Otárola-Castillo 2013). Procrustes superimposition translates, scales, and rotates the coordinate data to allow for comparisons among objects (Gower 1975; Rohlf and Slice 1990). The *geomorph* package uses a partial Procrustes superimposition that projects the aligned specimens into tangent space subsequent to alignment in preparation for the use of multivariate methods that assume linear space (Rohlf 1999; Slice 2001).

Principal components analysis (Jolliffee 2002) was used as an exploratory means of visualizing shape variation among the bottles. The shape changes described by each principal axis are commonly visualized using thin-plate spline warping of a reference 3D mesh (Klingenberg 2013; Sherratt et al. 2014). A residual randomization permutation procedure (RRPP; n=1000 permutations) was used for all Procrustes ANOVAs (Adams and Collyer 2015; Collyer and Adams 2018), which has higher statistical power and a greater ability to identify patterns in the data should they be present (Anderson and Ter Braak 2003). To assess whether shape differs by size (allometry) and site, Procrustes ANOVAs (Goodall 1991) were run that also enlist effect-sizes (z-scores) computed as standard deviates of the generated sampling distributions (Collyer et al. 2015). For the aggregated sample, a Procrustes ANOVA was run to assess whether shape changes with size, and the assumption of allometric slope homogeneity was tested with the *procD.allometry* function using the PredLine option (Adams and Nistri 2010). Should this test not be significant, then allometric slopes are similar—if not identical—across time and types.

A Procrustes ANOVA and pairwise test was used to identify sites where bottle shapes and types differ. The pairwise test is conceptually similar to trajectory analysis (Adams and Collyer 2007, 2009; Collyer and Adams 2007, 2013) in that pairwise statistics are vector lengths between vectors, but differs in that a factorial model is not explicitly needed to contrast vectors between point factor levels nested within group factor levels (Adams et al. 2017). Procrustes variance was used to discriminate between groups and to compare the amount of shape variation (morphological disparity) across communities (Zelditch et al. 2004), which is estimated as the Procrustes variance using residuals of linear model fit (Adams et al. 2017).

Morphological integration was assessed for the aggregated sample of whole vessels. Integration between pairs of traits was tested using a two-block partial least-squares (2B-PLS) analysis to evaluate relationships for two blocks of variables collected from the same specimens (Bookstein et al. 2003; Rohlf and Corti 2000; Wold 1966), using shape coordinates in all blocks of variables (Bastir and Rosas 2006; Bookstein et al. 2003; Gunz and Harvati 2007). To assess whether the different modules (RIM_{neck}, $NECK_{body}$, and $BODY_{base}$ in particular) are integrated, a two-sample test using effect sizes calculated as standard deviates in sampling distributions from the 2B-PLS analyses were used to determine the significance and strength of integration between the modules (Adams and Collyer 2016).

Results

The mean consensus configuration and Procrustes residuals were calculated using a generalized Procrustes analysis (GPA) (Figure 4). This initial view of the data demonstrates the degree of variability in Caddo bottles that occurs across the sample. As an exploratory measure, GM methods—to include GPA—aid in clarifying shape differences, and in the production of novel *a posteriori* hypotheses (Mitteroecker and Gunz 2009).

Principal components analysis (PCA) was conducted on scaled, translated, and rotated landmarks and semilandmarks, and demonstrates that the first two PC's account for 68 (PC1) and 27 (PC2) percent of the variation in bottle shape (Table 3 and Figure 6). Together, PC1 and PC2 account for 95 percent of shape variation, with all remaining PCs representing three or fewer percent of the variation (see Table 3). The first two PCs are plotted in Figure 5, where warp grids represent the shape changes along PC1 and PC2. This plot indicates that shape

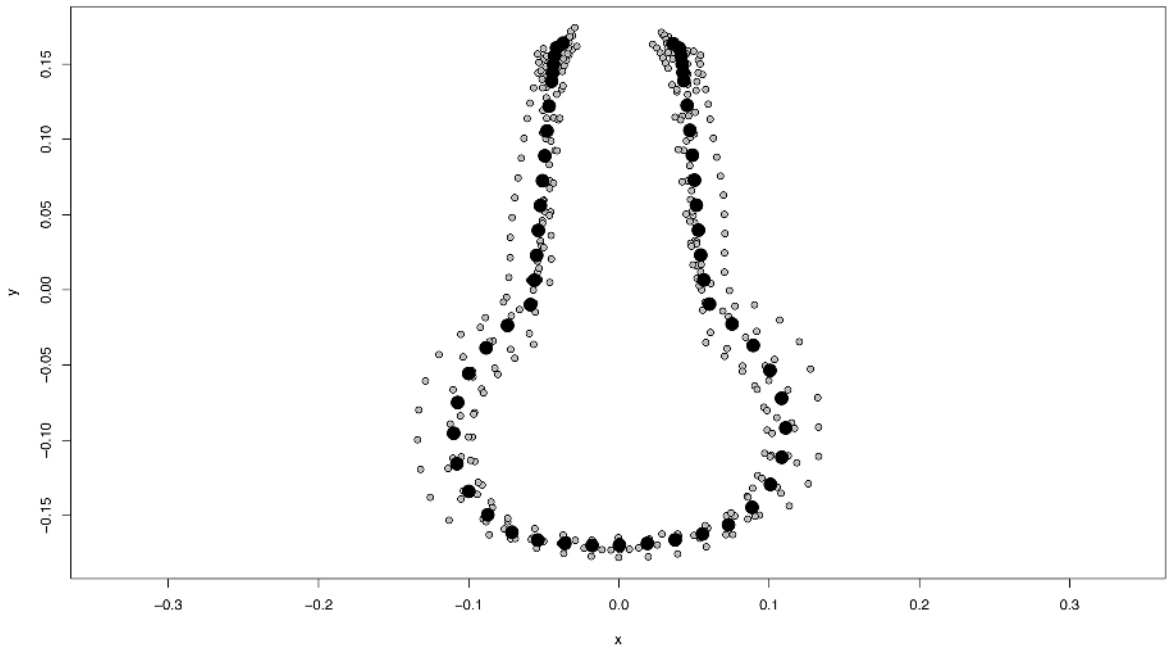

Figure 4. Results of generalized Procrustes analysis for Smithport Plain whole bottles. Mean consensus configuration shown in black; samples in gray.

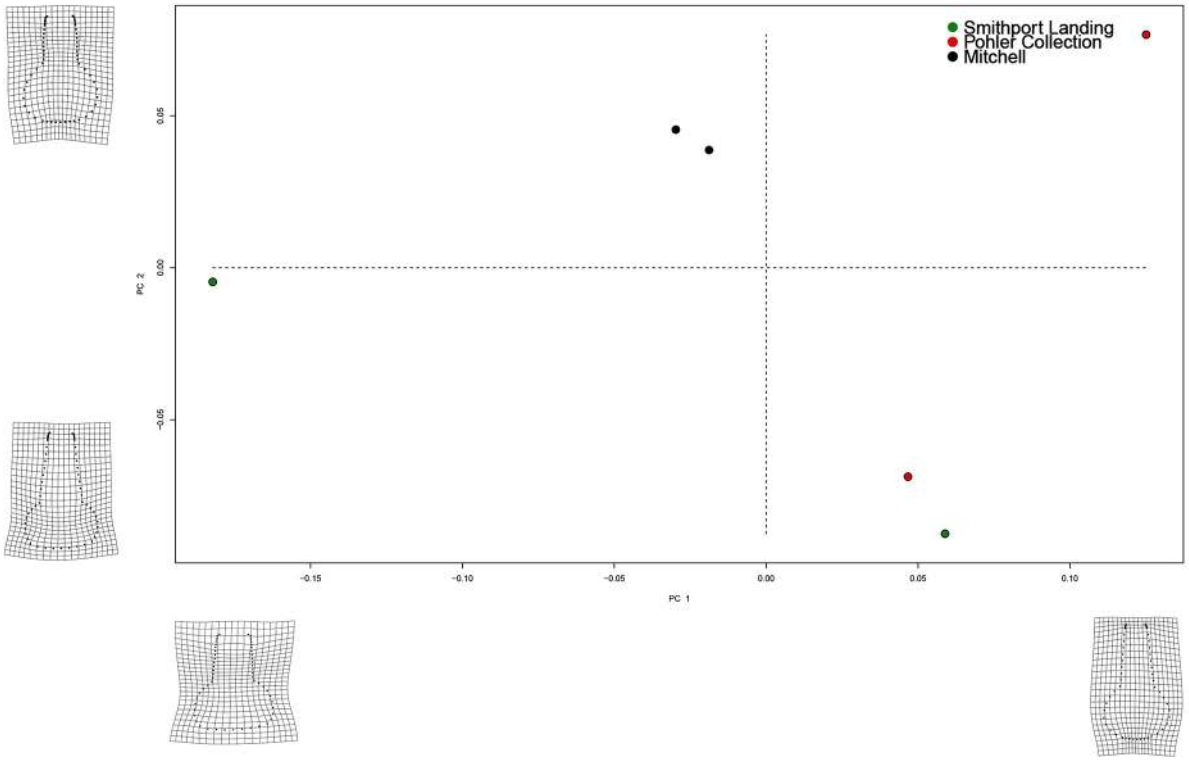

Figure 5. Results of PCA summarizing shape variation in the whole bottle sample.

Table 3. Results of PCA.

	SD	PV	CP
PC1	0.106	0.683	0.683
PC2	0.066	0.268	0.951
PC3	0.023	0.033	0.985
PC4	0.014	0.013	0.997
PC5	0.007	0.003	1.000

SD = standard deviation; PV = proportion of variance; CVE = cumulative proportion.

changes associated with PC1 articulate most readily with base and body shape, and shape changes associated with PC2 articulate with base, body, and neck shape.

A Procrustes ANOVA was used to test for significant allometry. Results of the ANOVA indicate significant allometry in the sample (RRPP = 1000, Rsq = 0.59427, Pr(>F) = 0.0075), indicating that Smithport Plain bottle shapes change with size. A Procrustes ANOVA was used to test for a significant difference in bottle shape by site, and results indicate that there is not a significant difference in bottle shape by site (RRPP = 1000, Rsq = 0.40907, Pr(>F) = 0.537).

Bottle base and body morphology

Two Smithport Plain bottles, specimen numbers 405 and 430, from Burials 11 and 12 at the Belcher Mound site are missing the upper portions of the neck and rim, and therefore could not be included in the analysis of whole vessels. Using a subset of the same constellation of landmarks and equidistant semilandmarks from the analysis of whole vessels (landmarks/semilandmarks 15-41), these two samples were added for an analysis of bottle base and body morphology. The mean consensus configuration and Procrustes residuals were calculated using a GPA for the base and body sample (Figure 6).

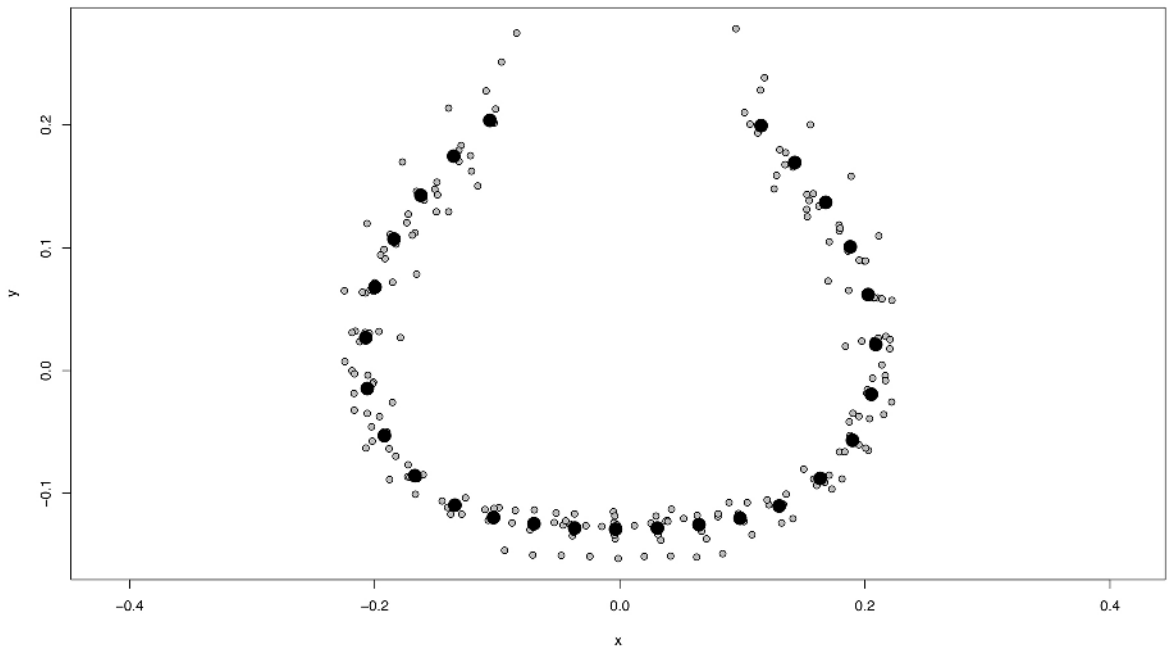

Figure 6. Results of generalized Procrustes analysis for Smithport Plain base and body sample. Mean consensus configuration shown in black; samples in gray.

PCA was conducted on scaled, translated, and rotated landmarks and semilandmarks, and demonstrates that the first two PCs account for 83 (PC1) and 15 (PC2) percent of the variation in bottle base and body shape (Table 4 and Figure 8). Together, PC1 and PC2 account for 98 percent of the variation for base and body shape, with each remaining PC representing less than two percent of the variation (see Table 4). The first two PCs are plotted in Figure 7, where warp grids represent the shape changes along PC1 and PC2. The plot indicates that shape changes associated with PC1 articulate most readily with a tall, pear-shaped body and narrow base at the maximum, and a shorter, globular body and wide base at the minimum. For PC2, the maximum values articulate with a pear-shaped body that is widest near a broad base, and a shorter, globular body with a narrow and rounded base at the minimum.

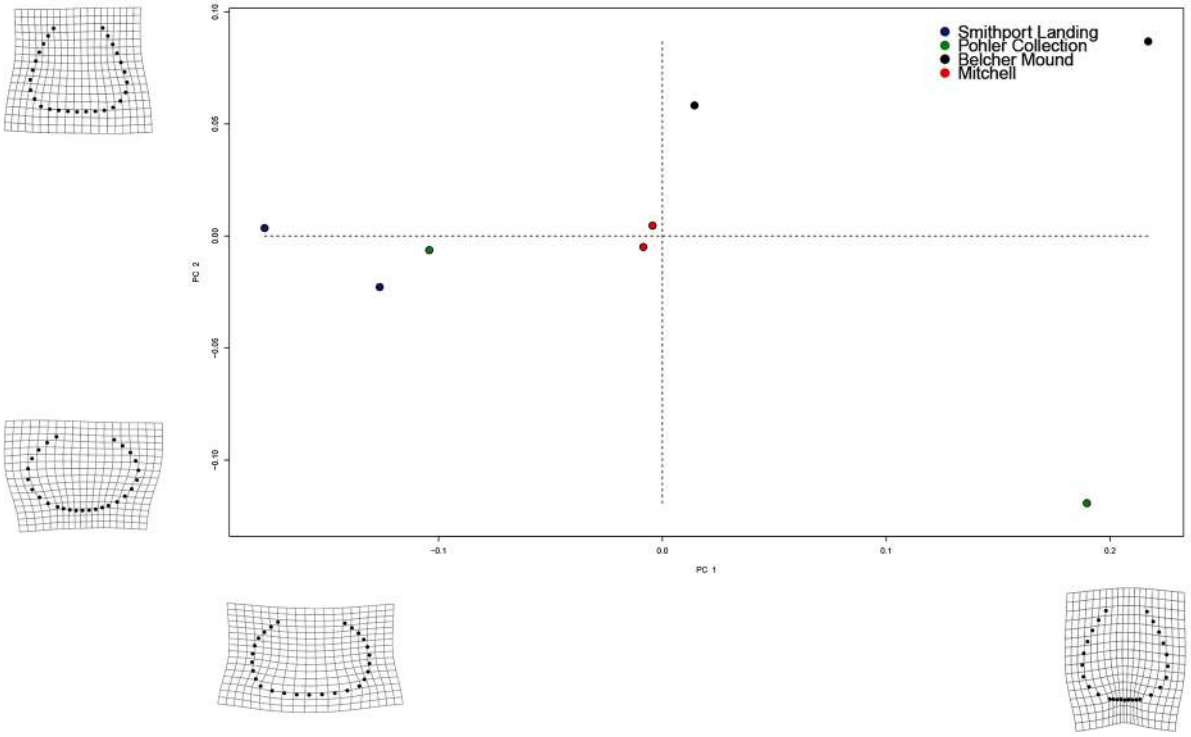

Figure 7. Results of PCA summarizing shape variation in the base and body sample.

Table 4. Results of PCA.

	SD	PV	CP
PC1	0.142	0.826	0.826
PC2	0.061	0.150	0.976
PC3	0.020	0.017	0.993
PC4	0.009	0.003	0.996
PC5	0.006	0.002	0.998
PC6	0.005	0.001	0.999
PC7	0.004	0.001	1.000

SD = standard deviation; PV = proportion of variance; CVE = cumulative proportion.

A Procrustes ANOVA was used to test for significant allometry. Results of the ANOVA indicate that allometry is not significant in the base and body sample (RRPP = 1000, Rsq = 0.17667, Pr(>F) = 0.275). A second Procrustes ANOVA was used to test for a significant difference in bottle shape by site. The advanced Procrustes ANOVA and pairwise test demonstrates a significant difference between Smithport Plain bottles from the Smithport Landing and Belcher Mound sites (Table 5).

Synthesis with aggregated sample

The Smithport Plain bottles were then added to the aggregated sample (see Table 1), omitting the two previously mentioned incomplete specimens (405 and 430). The aggregated sample of whole vessels (n=45) consists of five Caddo bottle types from 12 sites curated across five repositories in three states, with iterative analytical improvements achieved as new samples are added. The mean consensus configuration and Procrustes residuals were calculated using a GPA for the aggregated sample (Figure 8).

PCA was conducted on scaled, translated, and rotated landmarks and semilandmarks, and demonstrates that the first two PCs account for 59 (PC1) and 20 (PC2) percent of the variation in bottle shape (Table 6 and Figure 9). Together, PC1 and PC2 account for 79 percent of the variation in bottle shape, with each remaining PC representing ≤10 percent of the variation. The first two PCs are plotted in Figure 9, where warp grids represent the shape changes along PC1 and PC2. The plot indicates that shape changes associated with PC1 articulate with relative differences in base, body, neck, and rim shapes. Differences include a sharp or diffuse angle at the base and body juncture, flat versus slightly convex geometry, and a difference in relative width. Body differences range from globular to sub-globular, necks from everted to tapering, and rims from everted to slightly inverted. Shape changes associated with PC2 articulate with differences in relative base width, and a slightly carinated to globular body shape. In addition to a difference in relative width, the bottle necks also range from direct to slightly tapering, with rims that are vertical to slightly everted.

A Procrustes ANOVA was used to test for allometry, and significant allometry was identified in this sample (RRPP = 1000, Rsq = 0.18337, Pr(>F) = 0.001). Plots of predicted allometric trajectories for period (Formative-Early and Late-Historic Caddo) and type factors are presented in Figure 10. The null hypothesis of parallel slopes is rejected by the homogeneity of slopes test for group allometries, as the allometric trajectories differ significantly by period (RRPP = 1000, Rsq = 0.03711, Pr(>F) = 0.010). Allometric trajectories also differ significantly by type (RRPP = 1000, Rsq = 0.10182,

Table 5. Results of advanced Procrustes ANOVA and pairwise test (RRPP = 1000) of Smithport Plain bottle shape by site.

	Belcher Mound	Mitchell	Pohler Coll	Smithport Landing
Belcher Mound	0			
	0			
	1.000			
Mitchell	0.143	0		
	0.040	0		
	0.431	1.000		
Pohler Coll	0.155	0.086	0	
	0.172	-0.816	0	
	0.362	0.785	1.000	
Smithport Landing	0.280	0.147	0.203	0
	2.010	0.105	0.945	0
	0.032	0.393	0.183	1.000

Least-squares means distance matrix (top), effect sizes (middle), and P-values (bottom--significant results in bold).

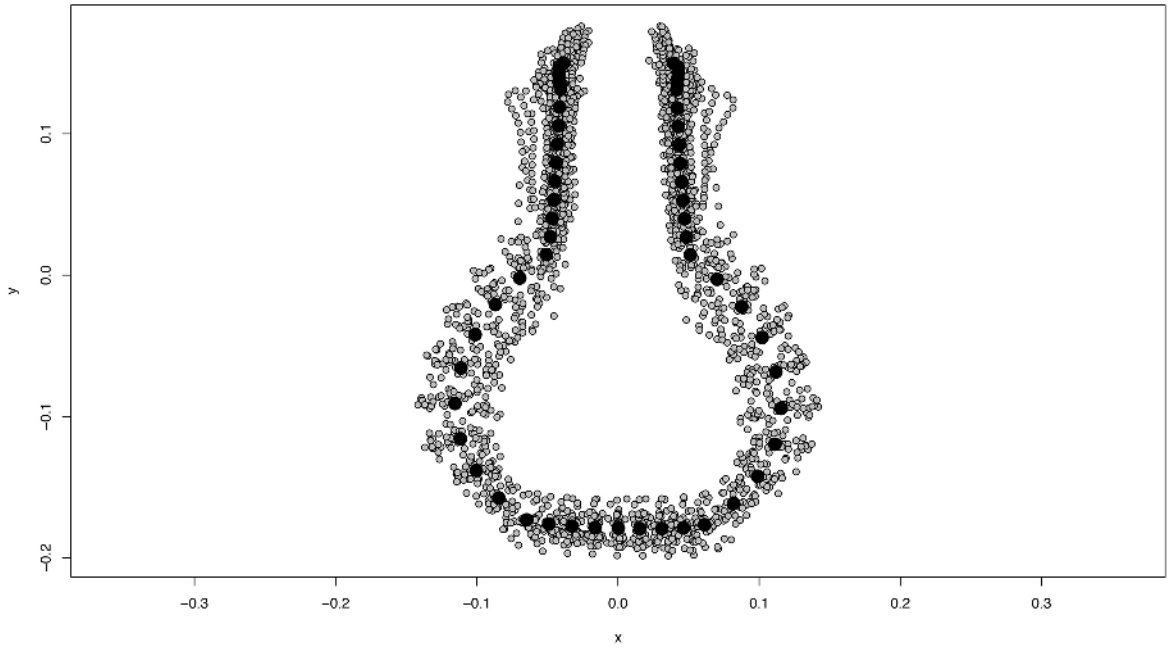

Figure 8. Results of generalized Procrustes analysis for the aggregated sample. Mean consensus configuration shown in black; samples in gray.

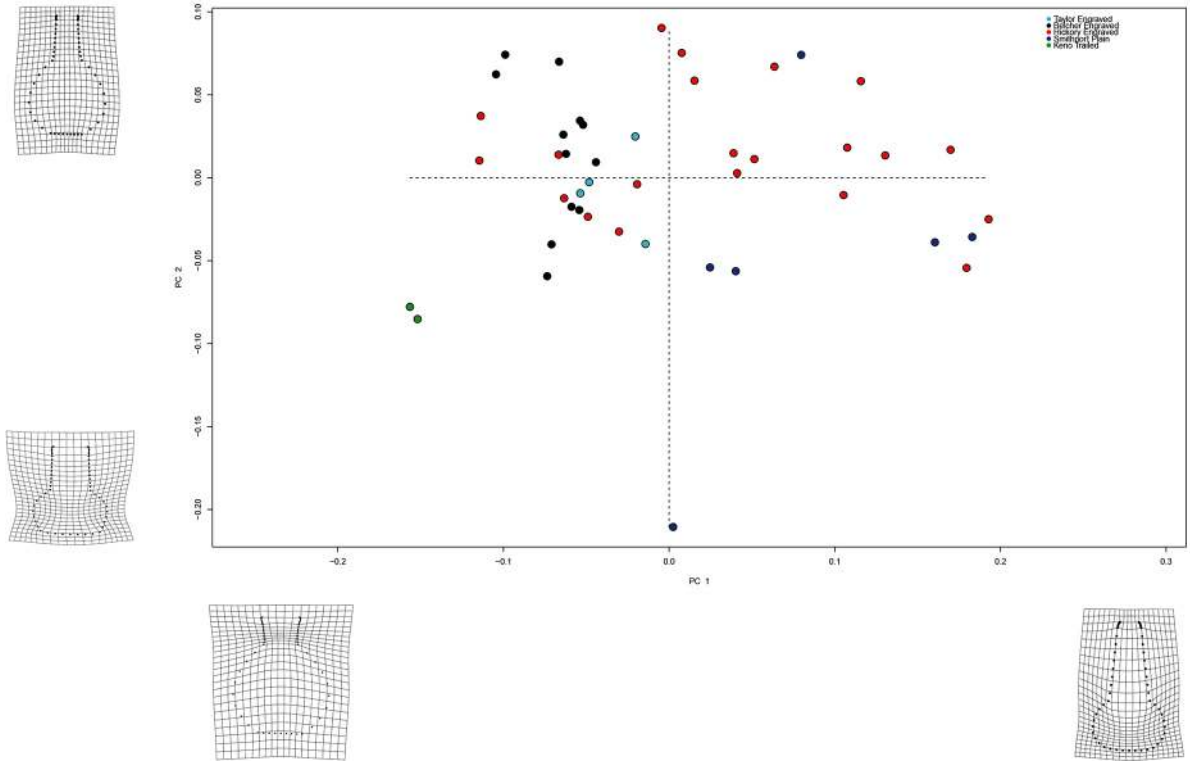

Figure 9. Results of PCA summarizing shape variation in the aggregated sample.

Table 6. Results of PCA.

	SD	PV	CP
PC1	0.093	0.592	0.592
PC2	0.055	0.205	0.797
PC3	0.038	0.100	0.897
PC4	0.026	0.045	0.942
PC5	0.018	0.022	0.964
PC6	0.013	0.011	0.975
PC7	0.010	0.007	0.982
PC8	0.008	0.004	0.986
PC9	0.007	0.004	0.990
PC10	0.006	0.003	0.993

SD = standard deviation; PV = proportion of variance; CVE = cumulative proportion.

Pr(>F) = 0.001) (see Figure 10), and the size of Formative-Early bottles, specifically those of the Hickory Engraved type, extends beyond the range of the Late-Historic and Smithport Plain types.

A second Procrustes ANOVA was used to test for a difference in bottle shape by site, which is (RRPP = 1000, Rsq = 0.52213, Pr(>F) = 0.001). An advanced Procrustes ANOVA and pairwise comparison was used to identify those sites where bottle assemblages differ, and whether that difference is in magnitude, direction, or both (Table 7). Those sites with bottle samples found to differ significantly include Belcher Mound compared to Gahagan Mound, Smithport Landing, Haley Place, Mitchell, and the Pohler Collection. In addition, Smithport Landing also differs significantly compared to Haley Place, and Mitchell.

A third Procrustes ANOVA was used to test for a difference in bottle shape by type, which is significant (RRPP = 1000, Rsq = 0.3907, Pr(>F) = 0.001). An advanced Procrustes ANOVA and pairwise comparison was used to identify which bottle types differ and whether that difference is in magnitude, direction, or both (Table 8). Those bottle types found to differ significantly include Keno Trailed compared to Belcher Engraved, Hickory Engraved, Smithport Plain, and Taylor Engraved; also Belcher Engraved compared to Hickory Engraved, and Smithport Plain; and finally, Smithport Plain compared to Taylor Engraved.

A test of morphological disparity indicates that Hickory Engraved and Smithport Plain bottles display a greater range of shape variation among individual bottles relative to other groups, and differ significantly from the Belcher Engraved, Keno Trailed, and Taylor Engraved bottles (Table 9). This indicates that the Formative-Early Caddo bottles may encompass a greater range of morphological variability than the Late-Historic Caddo bottles in the sample; an assertion that was later confirmed in a subsequent test of morphological disparity by period (Table 10).

The 2B-PLS analyses, each enlisting 1000 random permutations, was used to test for morphological integration between combinations of bottle components (rim, neck, body, and base). The results indicate significant integration between the rim and neck (r_{PLS} = 0.969, P-value = 0.001), rim and body (r_{PLS} = 0.942, P-value = 0.001), rim and base (r_{PLS} = 0.663, P-value = 0.001), neck and body (r_{PLS} = 0.962, P-value = 0.001), neck and base (r_{PLS} = 0.869, P-value = 0.001), and the body and base (r_{PLS} = 0.859, P-value = 0.001) for bottles in the sample (Figure 11). A pairwise test of morphological integration was used to identify combinations of traits that covary. Results indicate that for this sample of Caddo bottles, the RIM_{neck} and RIM_{base}, RIM_{body} and RIM_{base}, and RIM_{base} and $NECK_{body}$ are significantly integrated (Table 11).

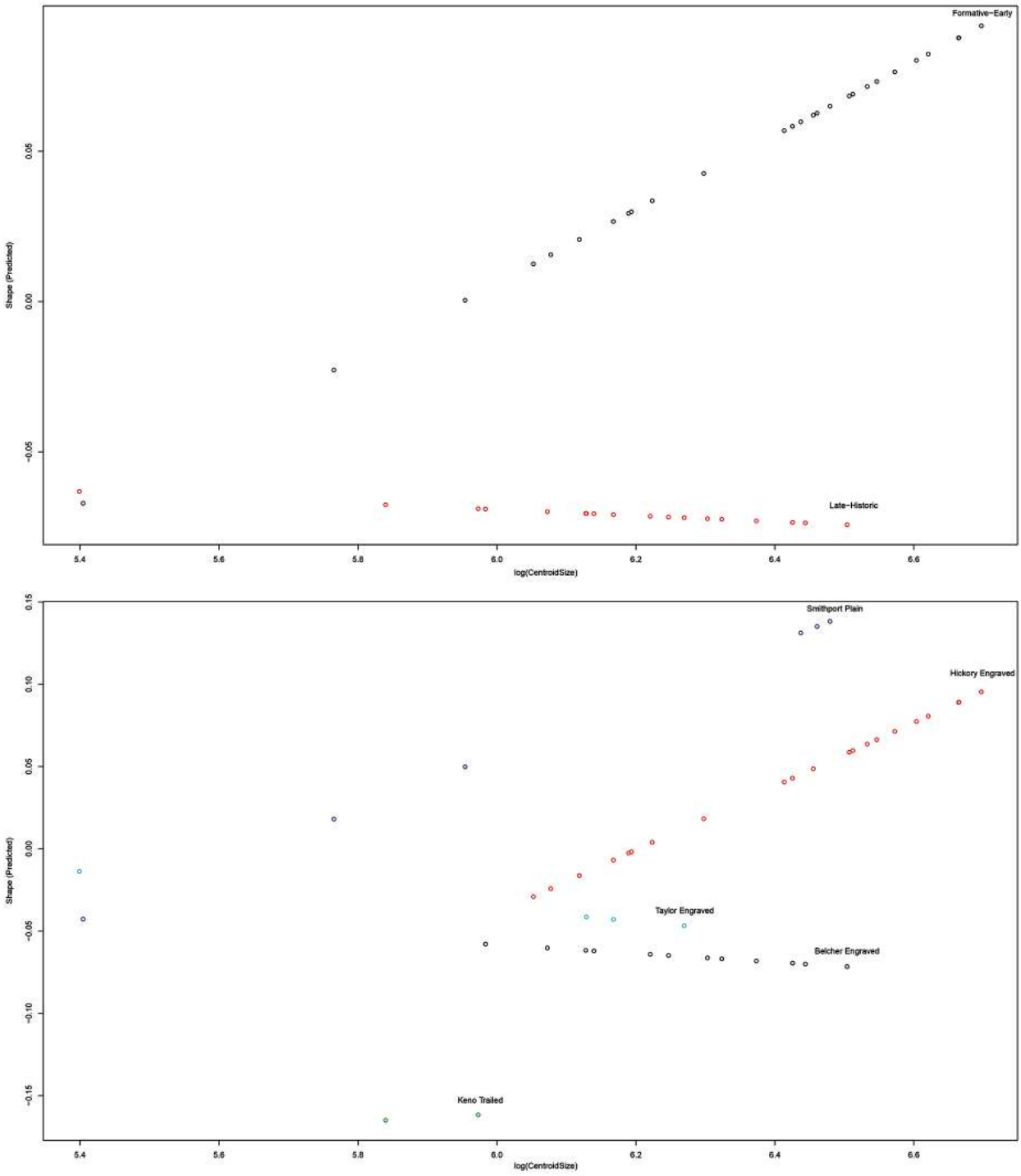

Figure 10. Predicted values of Caddo bottle shape from temporal (top) and type (bottom) regressions versus log(CentroidSize).

Table 7. Least-squares mean distance matrix (top), effect sizes (middle), and P-values (bottom) for advanced Procrustes ANOVA and pairwise test (RRPP = 1000) of bottle shape by site.

	Allen	Belcher	Crenshaw	FNF	Gahagan	GCD	Haley	Hatchel	MCM	Mitchell	Pohler	Smithport
Allen	0											
	0											
	1.000											
Belcher	0.181	0										
	1.478	0										
	0.118	1.000										
Crenshaw	0.161	0.132	0									
	0.059	0.333	0									
	0.433	0.319	1.000									
FNF	0.070	0.204	0.147	0								
	-1.289	1.870	-0.117	0								
	0.930	0.075	0.488	1.000								
Gahagan	0.096	0.251	0.218	0.092	0							
	-0.672	4.902	1.382	-0.754	0							
	0.706	**0.001**	0.101	0.756	1.000							
GCD	0.150	0.127	0.057	0.143	0.203	0						
	-0.060	0.278	-1.470	-0.197	1.211	0						
	0.455	0.328	0.954	0.513	0.138	1.000						
Haley	0.134	0.092	0.066	0.134	0.202	0.068	0					
	0.313	1.598	-1.095	0.190	2.739	-1.072	0					
	0.303	0.078	0.894	0.337	**0.013**	0.899	1.000					
Hatchel	0.117	0.202	0.121	0.067	0.129	0.121	0.127	0				
	-0.531	1.830	-0.507	-1.307	-0.081	-0.496	0.106	0				
	0.652	0.069	0.648	0.915	0.457	0.632	0.378	1.000				
MCM	0.116	0.139	0.151	0.135	0.142	0.122	0.124	0.140	0			
	-0.593	0.509	-0.124	-0.321	0.110	-0.521	0.033	-0.246	0			
	0.693	0.279	0.511	0.559	0.400	0.665	0.382	0.546	1.000			
Mitchell	0.131	0.064	0.096	0.146	0.201	0.087	0.040	0.148	0.107	0		
	0.188	0.376	-0.503	0.473	2.942	-0.630	-1.029	0.527	-0.273	0		
	0.368	0.308	0.624	0.268	**0.007**	0.697	0.849	0.264	0.531	1.000		
Pohler	0.115	0.092	0.088	0.124	0.175	0.070	0.048	0.124	0.079	0.040	0	
	-0.196	1.178	-0.722	-0.034	1.969	-1.020	-0.874	-0.034	-0.866	-1.186	0	
	0.493	0.124	0.742	0.433	**0.046**	0.869	0.813	0.440	0.809	0.924	1.000	
Smithport	0.075	0.200	0.195	0.094	0.105	0.177	0.153	0.144	0.133	0.147	0.136	0
	-0.942	5.374	1.298	-0.634	0.241	1.000	2.435	0.348	0.160	2.315	1.668	0
	0.849	**0.001**	0.138	0.683	0.354	0.163	**0.026**	0.309	0.370	**0.027**	0.072	1.000

Significant results in bold; FNF = Frank Norris Farm, GCD = George C. Davis, MCM = Mustang Creek Mound.

Table 8. Least-squares mean distance matrix (top), effect sizes (middle), and P-values (bottom) for advanced Procrustes ANOVA and pairwise test (RRPP = 1000) of bottle shape by type

	Belcher Eng	HE	Keno Tr	Smithport Pl	Taylor Eng
Belcher Engraved	0				
	0				
	1.000				
Hickory Engraved	0.114	0			
	4.499	0			
	0.002	1.000			
Keno Trailed	0.171	0.226	0		
	2.449	4.131	0		
	0.023	**0.001**	1.000		
Smithport Plain	0.168	0.085	0.251	0	
	4.812	1.589	4.133	0	
	0.002	0.071	**0.001**	1.000	
Taylor Engraved	0.046	0.085	0.176	0.130	0
	-0.738	0.932	1.931	2.021	0
	0.745	0.184	**0.049**	**0.034**	1.000

Significant results in bold.

Table 9. Pairwise absolute differences between variances (top) and P-values (bottom) for the test of morphological disparity by type.

	Belcher Eng	HE	Keno Tr	Smithport Pl	Taylor Eng
Belcher Engraved	0				
	1.000				
Hickory Engraved	0.009	0			
	0.004	1.000			
Keno Trailed	0.001	0.010	0		
	0.906	0.082	1.000		
Smithport Plain	0.011	0.002	0.012	0	
	0.015	0.698	0.093	1.000	
Taylor Engraved	0.001	0.008	0.002	0.009	0
	0.827	0.088	0.760	0.080	1.000

Significant results in bold, RRPP = 1000.

Table 10. Pairwise absolute differences between variances (top) and P-values (bottom) for the test of morphological disparity by time period.

	Formative-Early	Late-Historic
Formative-Early	0	
	1.000	
Late-Historic	0.007	0
	0.007	1.000

Significant results in bold, RRPP = 1000.

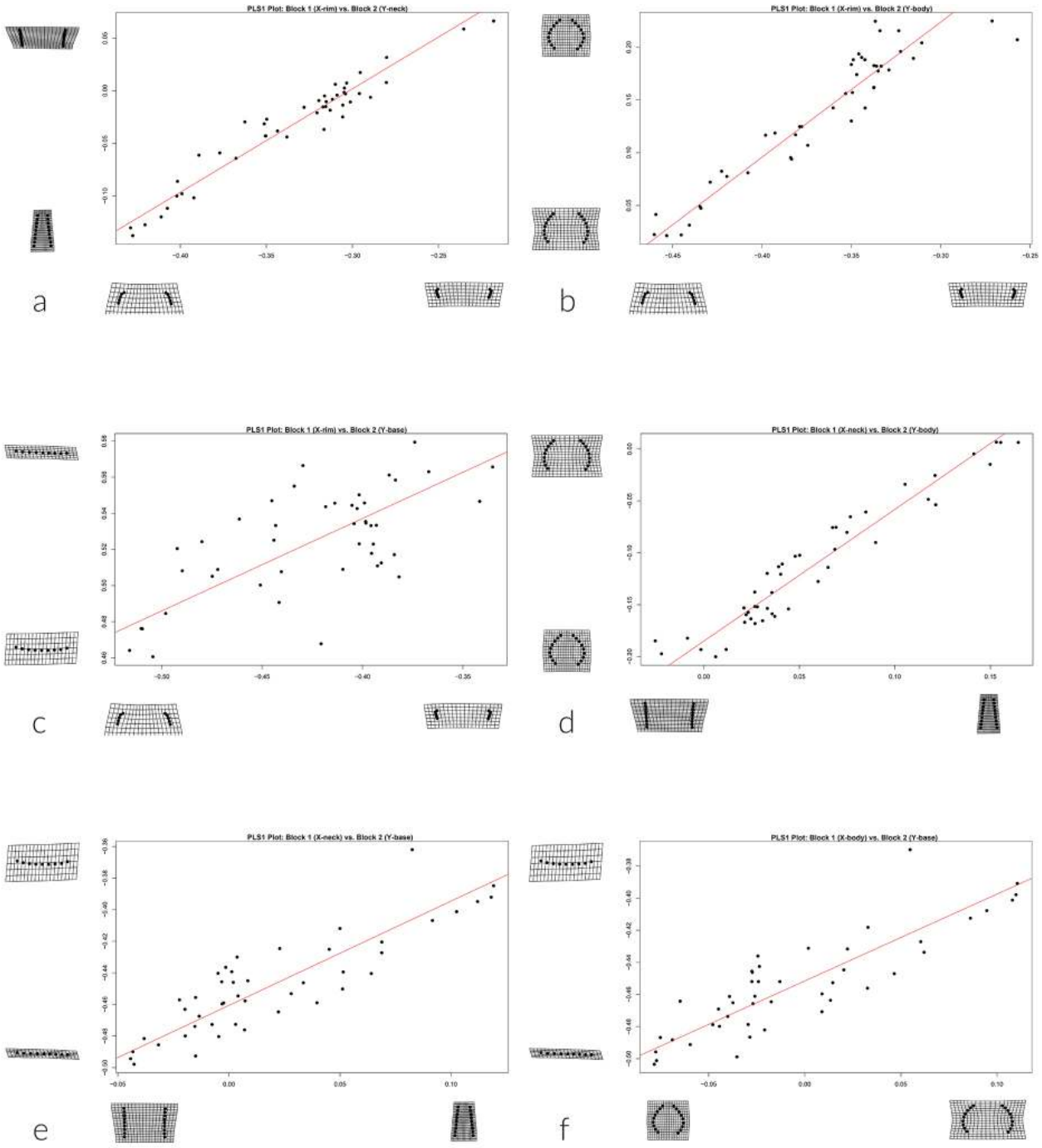

Figure 11. Results of 2B-PLS analyses for pairs of morphological components; (a) rim and neck, (b) rim and body, (c) rim and base, (d) neck and body, (e) neck and base, and (f) body and base.

Table 11. Comparison of morphological integration between modules.

Z	RIM_{neck}	RIM_{body}	RIM_{base}	$NECK_{body}$	$NECK_{base}$	$BODY_{base}$
RIM_{neck}	0					
RIM_{body}	0.451	0				
RIM_{base}	2.727	2.401	0			
$NECK_{body}$	0.493	0.048	2.331	0		
$NECK_{base}$	1.120	0.726	1.566	0.674	0	
$BODY_{base}$	1.424	1.030	1.362	0.972	0.258	0

P	RIM_{neck}	RIM_{body}	RIM_{base}	$NECK_{body}$	$NECK_{base}$	$BODY_{base}$
RIM_{neck}	1.000					
RIM_{body}	0.326	1.000				
RIM_{base}	**0.003**	**0.008**	1.000			
$NECK_{body}$	0.311	0.481	0.**010**	1.000		
$NECK_{base}$	0.131	0.234	0.059	0.250	1.000	
$BODY_{base}$	0.077	0.152	0.087	0.165	0.398	1.000

Matrix of pairwise differences in PLS effect sizes (left), and their associated significance levels (right).

Discussion and Conclusion

This repository-based analysis of a curated and majority-NAGPRA collection of intact or reconstructed Caddo bottles resulted in an improved characterization of Caddo bottle shapes, while highlighting similarities, differences, and a general trend toward standardization for the aggregated sample. Specifically, it resulted in a test of Smithport Plain bottle shapes confirming that discrete morphological characteristics (body and base) differ significantly between the Belcher Mound and Smithport Landing sites, supporting the morphological assertion initially posited by Webb (1959). The test included an analysis of Smithport Plain bottles from the Pohler Collection and Mitchell site, which do not differ significantly in shape from those recovered at the Smithport Landing or Belcher Mound sites. Analysis of the aggregate sample indicates allometric trajectories that are not homogenous for Formative-Early and Late-Historic Caddo types, a significant difference in bottle shape by site and type, significant morphological disparity between the Formative-Early and Late-Historic Caddo types, and significant morphological integration of pairs and suites of bottle components.

In the aggregated sample, significant assemblage-level differences in bottle shape exist between Belcher Mound compared with Gahagan Mound and Smithport Landing, Gahagan Mound compared with Haley Place, Mitchell, Pohler Collection, Haley Place and Smithport Landing, and Mitchell compared with those from Smithport Landing (see Table 7 and Figure 12). The results imply that bottle shapes employed by Formative-Early Caddo potters differ from those produced by Late-Caddo potters; an assertion echoed by the analyses of allometric trajectories (see Figure 10) and morphological disparity (see Table 10). While only a small sample has been examined thus far, the results of morphological disparity by period highlight a gradual trend toward standardization, where bottles produced in the Late-Historic Caddo periods occupy a more restricted range of morphospace than those manufactured in the Formative-Early Caddo periods. This dynamic assertion is subject to change as more bottles are added to the analysis.

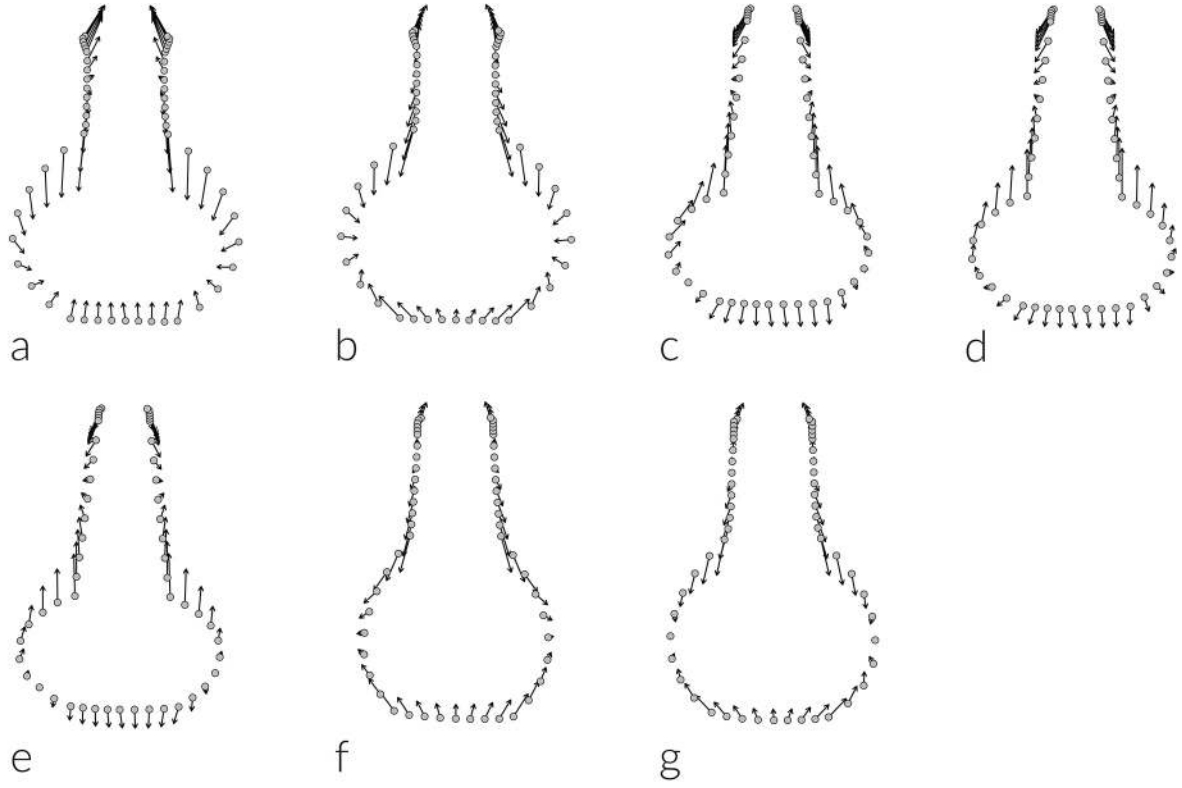

Figure 12. Comparison of mean bottle shapes by site for those sites found to differ significantly; (a) Belcher Mound (gray) and Gahagan Mound, (b) Belcher Mound (gray) and Smithport Landing, (c) Gahagan Mound (gray) and Haley Place, (d) Gahagan Mound (gray) and Mitchell, (e) Gahagan Mound (gray) and Pohler, (f) Haley Place (gray) and Smithport Landing, and (g) Mitchell (gray) and Smithport Landing.

Significant type-specific differences in bottle shape occur between Belcher Engraved compared with Hickory Engraved, Keno Trailed, and Smithport Plain; Keno Trailed compared with Smithport Plain and Taylor Engraved; Hickory Engraved compared with Keno Trailed; and Smithport Plain compared with Taylor Engraved (see Table 8 and Figure 13). The test of morphological disparity indicated that Hickory Engraved and Smithport Plain bottles occupy a significantly greater range of morphospace than the Belcher Engraved bottles (see Table 9). Elsewhere it may be the case that dimensional attributes are inappropriate for use in studies of standardization and diversity (Rice 1991); however, the morphological disparity results suggest a high degree of utility in clarifying questions of standardization and diversity through the employment of morphological traits associated with Caddo bottles. This can, in turn, provide evidence for varying degrees of tolerance in production, where a higher tolerance yields a greater range of variation in shape that decreases as shapes become more standardized (Eerkins and Bettinger 2001). In this sample, the tolerance for diversity in Caddo bottle shape is higher in the Formative-Early Caddo period, and becomes more restricted through time. Results specify that the tolerance for variation in Caddo bottle shapes is greater in the case of Smithport Plain and Hickory Engraved than it is for Belcher Engraved.

Results from the test of morphological integration indicate that Caddo bottles are significantly integrated (see Figure 11), lending some support to the hypothesis that Caddo potters were adhering to a template of vessel shape associated with specific decorative motifs (Early 2012). However, the suites of attributes were not found to covary in a predicted manner, as it is the RIM_{neck} and RIM_{base}, RIM_{body} and RIM_{base}, and RIM_{base} and $NECK_{body}$ that exhibit significant integration (see Table 11). An important component of the expanded research program will be type-specific tests of morphological integration following an increase in sample size.

The significant difference in the production of Smithport Plain body and base shapes at the

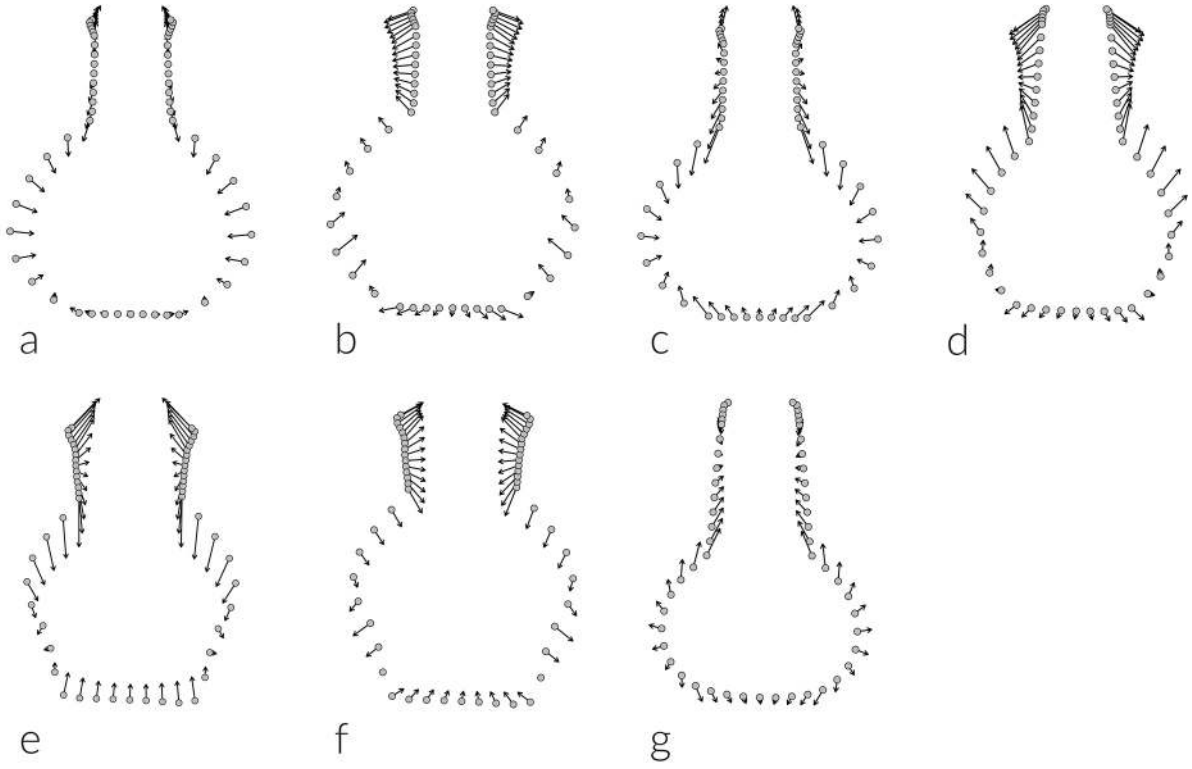

Figure 13. Comparison of mean bottle shapes by type for those types found to differ significantly; (a) Belcher Engraved (gray) and Hickory Engraved, (b) Belcher Engraved (gray) and Keno Trailed, (c) Belcher Engraved (gray) and Smithport Plain, (d) Hickory Engraved (gray) and Keno Trailed, (e) Keno Trailed (gray) and Smithport Plain, (f) Keno Trailed (gray) and Taylor Engraved, and (g) Smithport Plain (gray) and Taylor Engraved.

Smithport Landing and Belcher Mound sites was posited in the initial analysis (Selden, Jr. 2018a) where the differences in shape were seen as a possible north-south transition for the combined sample of Hickory Engraved and Smithport Plain types. In comparing these results with a recent analysis of the Hickory Engraved sample (Selden, Jr. 2018b), it is evident that while these two Formative-Early Caddo types exhibit similar morphological differences over geographic space, the differences are dynamic and will be further clarified by the continued and iterative expansion of type-specific analyses.

The contribution of GM methods to questions of Caddo ceramic morphology holds substantial promise. Those results presented here provide a succinct preview of a rigorous and systematic research design that capitalizes on the variability of Caddo ceramic shapes through an analysis of type-specific (Smithport Plain) morphology that is followed by an analysis of the aggregated sample of Caddo bottles. Iterative improvements to this research program will continue as new specimens are made available and incorporated. That progression will include the addition of Caddo bottles from the Bison B site in northwest Louisiana (Woodall 1969) curated at Southern Methodist University, and an expansion of the Belcher and Taylor Engraved samples. This will test whether similarity in Late-Historic Caddo bottle shape is a local, regional, or area-wide trend. Also considered will be the continued analyses of morphological disparity between different temporal periods to test whether significant morphological disparity and allometry between the temporal periods varies elsewhere; and the continued use of morphological integration to identify which of those morphological traits associated with Caddo bottle production might be said to covary.

Acknowledgments. I extend my gratitude to the Caddo Nation of Oklahoma, the Williamson Museum at Northwestern State University, the Louisiana State Exhibit Museum, the Texas Archeological Research Laboratory, and the Louisiana State University (LSU) Museum of Natural Science for the requisite permissions and access needed to generate the 3D scans of the Caddo bottles. Thanks also to Dean C. Adams, Emma Sherratt, Stephen J. Lycett, Michael J. Shott, Timothy K. Perttula, Hiram F. (Pete) Gregory, Jeffrey S. Girard, and Kersten Bergstrom for their constructive criticisms, comments, and suggestions throughout the development of this research design, to the editors for their invitation to submit, and the anonymous reviewers whose comments improved the manuscript. Development of the analytical work flow and production of 3D scans from the Clarence H. Webb collection was funded by a grant to the author (P14AP00138) from the National Center for Preservation Technology and Training. Production of 3D scans for repatriated Caddo bottles from the Crenshaw Mound and the Pohler Collection was funded by a grant to the author by the Caddo Nation of Oklahoma.

References Cited

Adams, Dean C. and Michael L. Collyer
2007 Analysis of Character Divergence along Environmental Gradients and other Covariates. *Evolution* 61(3):510-515.

2009 A General Framework for the Analysis of Phenotypic Trajectories in Evolutionary Studies. *Evolution* 63(5):1143-1154.

2015 Permutation Tests for Phylogenetic Comparative Analyses of High-Dimensional Shape Data: What you Shuffle Matters. *Evolution* 69(3):823-829.

2016 On the Comparison of the Strength of Morphological Integration across Morphometric Datasets. *Evolution* 70(11):2623-2631.

Adams, Dean C., Michael L. Collyer, Antigoni Kaliontzopoulou and Emma Sherratt
2017 Package 'geomorph': Geometric Morphometric Analyses of 2D/3D Landmark Data. R package version 3.0.5.

Adams, Dean C. and Annamaria Nistri
2010 Ontogenetic Convergence and Evolution of Foot Morphology in European Cave Salamanders (Family: Plethodontidae). *BMC Evolutionary Biology* 10:1-10.

Adams, Dean C. and Erik Otárola-Castillo
2013 geomorph: An R Package for the Collection and Analysis of Geometric Morphometric Shape Data. *Methods in Ecology and Evolution* 4(4):393-399.

Adams, Dean C., F. James Rohlf and Dennis E. Slice
2004 Geometric Morphometrics: Ten Years of Progress following the 'Revolution'. *Italian Journal of Zoology* 71(1):5-16.

2013 A Field Comes of Age: Geometric Morphometrics in the 21st Century. *Hystrix* 24(1):7-14.

Anderson, Marti J. and Cajo J. F. Ter Braak
2003 Permutation Tests for Multi-Factoral Analysis of Variance. *Journal of Statistical Computation and Simulation* 73(2):85-113.

Archer, Will and David R. Braun
2010 Variability in Bifacial Technology at Elandsfontein, Western Cape, South Africa: A Geometric Morphometric Approach. *Journal of Archaeological Science* 37(1):201-209.

Archer, Will, Philipp Gunz, Karen L. van Niekerk, Christopher S. Henshilwood and Shannon P. McPherron
2015 Diachronic Change within the Still Bay at Blombos Cave, South Africa. *PLoS One* 10(7):e0132428.

Archer, Will, Cornel M. Pop, Philipp Gunz and Shannon P. McPherron
2016 What is Still Bay? Human Biogeography and Bifacial Point Variability. *Journal of Human Evolution* 97:58-72.

Archer, Will, Cornel M. Pop, Zeljko Rezek, Stefan Schlager, Sam C. Lin, Marcel Weiss, Tamara Dogandžić, Dawit Desta and Shannon P. McPherron
2017 A Geometric Morphometric Relationship Predicts Stone Flake Shape and Size Variability. *Archaeological and Anthropological Sciences* 10.1007/s12520-017-0517-2.

Barceló, Juan A.
2010 Visual Analysis in Archaeology. An Artificial Intelligence Approach. In *Morphometrics for Nonmorphometricians*, edited by A. M. T. Elewa, pp. 93-156. Springer Verlag, Heidelberg.

Bastir, M. and A. Rosas
2006 Correlated Variation between the Lateral Basicranium and the Face: A Geometric Morphometric Study in Different Human Groups. *Archives of Oral Biology* 51(9):814-824.

Birkhoff, George D.
1933 *Aesthetic Measure*. Harvard University Press, Cambridge.

Bookstein, Fred L.
1982 Foundations of Morphometrics. *Annual Review of Ecology and Systematics* 13:451-470.
1991 *Morphometric Tools for Landmark Data: Geometry and Biology*. Cambridge University Press, Cambridge.
2016 The Inappropriate Symmetries of Multivariate Statistical Analysis in Geometric Morphometrics. *Evolutionary Biology* 43:277-313.

Bookstein, Fred L., Philipp Gunz, Philipp Mitteræcker, Hermann Prossinger, Katrin Schæfer and Horst Seidler
2003 Cranial Integration in Homo: Singular Warps Analysis of the Midsagittal Plane in Ontogeny and Evolution. *Journal of Human Evolution* 44(2):167-187.

Bookstein, Fred L., Dennis E. Slice, Philipp Gunz and Philipp Mitteroecker
2004 Anthropology Takes Control of Morphometrics. *Collegium Antropologicum* 28(Suppl 2):121-132.

Buchanan, Briggs and Mark Collard
2010 A Geometric Morphometrics-Based Assessment of Blade Shape Differences among Paleoindian Projectile Point Types from Western North America. *Journal of Archaeological Science* 37(2):350-359.

Buchanan, Briggs, Mark Collard, Marcus J. Hamilton and Michael J. O'Brien
2011 Points and Prey: A Quantitative Test of the Hypothesis that Prey Size Influences Early Paleoindian Projectile Point Form. *Journal of Archaeological Science* 38(4):852-864.

Buchanan, Briggs, Metin I. Eren, Matthew T. Boulanger and Michael J. O'Brien
2015 Size, Shape, Scars, and Spatial Patterning: A Quantitative Assessment of Late Pleistocene (Clovis) Point Resharpening. *Journal of Archaeological Science: Reports* 3:11-21.

Buchanan, Briggs, Eileen Johnson, Richard E. Strauss and Patrick J. Lewis
2007 A Morphometric Approach to Assessing Late Paleoindian Projectile Point Variability on the Southern High Plains. *Plains Anthropologist* 52(203):279-299.

Buchanan, Briggs, Michael J. O'Brien and Mark Collard
2013 Continent-Wide or Region-Specific? A Geometric Morphometrics-Based Assessment of Variation in Clovis Point Shape. *Archaeological and Anthropological Sciences* 6(2):145-162.

Byrne, Fergus, Tomos Proffitt, Adrian Arroyo and Ignacio de la Torre
2016 A Comparative Analysis of Bipolar and Freehand Experimental Knapping Products from Olduvai Gorge, Tanzania. *Quaternary International* 424:58-68.

Cardillo, Marcelo, Judith Charlin and Karen Borrazzo
2010 Una Exploración de la Variación Métrica y Morfológica en Instrumentos de Filo Largo en Patagonia Meridional. In *La Arqueometría en Argentina y Latinoamérica*, edited by S. Bertolino, G. R. Cattaneo and A. D. Izeta, pp. 147-152. Editorial de la FFyH, Universidad Nacional de Córdoba, Córdoba.

Caruana, Matthew V., Susana Carvalho, David R. Braun, Darya Presnyakova, Michael Haslam, Will Archer, Rene Bobe and John W. K. Harris
2014 Quantifying Traces of Tool Use: A Novel Morphometric Analysis of Damage Patterns on Percussive Tools. *PLoS One* 9(11):e113856.

Castiñeira, Carola, Marcelo Cardillo, Judith Charlin and Jorge Baeza
2011 Analisis de Morfometría Geométrica en Puntas Cola de Pescado del Uruguay. *Latin American Antiquity* 22(3):335-358.

Charlin, Judith, Marcelo Cardillo and Karen Borrazzo
2014 Spatial Patterns in Late Holocene Lithic Projectile Point Technology of Tierra del Fuego (Southern South America): Assessing Size and Shape Changes. *World Archaeology* 46(1):78-100.

Charlin, Judith and Rolando González-José
2012 Size and Shape Variation in Late Holocene Projectile Points of Southern Patagonia: A Geometric Morphometric Study. *American Antiquity* 77(2):221-242.

Chitwood, D. H.
2014 Imitation, genetic lineages, and time influenced the morphological evolution of the violin. *PLoS One* 9(10):e109229.

Collyer, Michael L. and Dean C. Adams
2007 Analysis of Two-State Multivariate Phenotypic Change in Ecological Studies. *Ecology* 88(3):683-692.
2013 Phenotypic Trajectory Analysis: Comparison of Shape Change Patterns in Evolution and Ecology. *Hystrix* 24(1):75-83.
2018 RRPP: An R Package for Fitting Linear Models to High-Dimensional Data using Residual Randomization. *Methods in Ecology and Evolution* https://doi.org/10.1111/2041-210X.13029.

Collyer, Michael L., David J. Sekora and Dean C. Adams
2015 A Method for Analysis of Phenotypic Change for Phenotypes Described by High-Dimensional Data. *Heredity* 115(4):357-365.

Corti, Marco
1993 Geometric Morphometrics: An Extension of the Revolution. *Trends in Ecology & Evolution* 8(8):302-303.

Costa, August G.
2010 A Geometric Morphometric Assessment of Plan Shape in Bone and Stone Acheulean Bifaces from the Middle Pleistocene Site of Castel di Guido, Latium, Italy. In *New Perspectives on Old Stones: Analytical Approaches to Paleolithic Technologies*, edited by S. J. Lycett and P. R. Chauhan, pp. 23-4110.1007/978-1-4419-6861-6_2. Springer, New York.

de Azevedo, Soledad, Judith Charlin and Rolando González-José
2014 Identifying Design and Reduction Effects on Lithic Projectile Point Shapes. *Journal of Archaeological Science* 41:297-307.

Early, A. M.
2012 Form and Structure in Prehistoric Caddo Pottery Design. In *The Archaeology of the Caddo*, edited by T. K. P. a. C. P. Walker, pp. pp. 26-46. University of Nebraska Press, Lincoln.

Eerkins, Jelmer W. and Robert L. Bettinger
2001 Techniques for Assessing Standardization in Artifact Assemblages: Can We Scale Material Variability? *American Antiquity* 66(3):493-504.

Elewa, Ashraf M. T.
2010 *Morphometrics for Nonmorphometricians*. Lecture Notes in Earth Sciences10.1007/978-3-540-95853-6. Springer, New York.

Eren, Metin I., Briggs Buchanan and Michael J. O'Brien
2015 Social Learning and Technological Evolution during the Clovis Colonization of the New World. *Journal of Human Evolution* 80:159-170.

Fox, Amy N.
2015 A Study of Late Woodland Projectile Point Typology in New York using Elliptical Fourier Outline Analysis. *Journal of Archaeological Science: Reports* 4:501-509.

Gadus, Eloise F.
2013 Twisted Serpents and Fierce Birds: Structural Variation in Caddo Engraved Ceramic Bottle Motifs. *Bulletin of the Texas Archeological Society* 84:213-245.

Gero, Joan and Jim Mazzullo
1984 Analysis of Artifact Shape Using Fourier Series in Closed Form. *Journal of Field Archaeology* 11(3):315.

Girrulat, Itaci Correa
2006 Contribution of Geometric Morphometrics to the Study of Archaeological Ceramics. *Revista Werken* 8:57-75.

Goodall, Colin
1991 Procrustes Methods in the Statistical Analysis of Shape. *Journal of the Royal Statistical Society. Series B (Methodological)* 53(2):285-339.

Gower, J. C.
1975 Generalized Procrustes Analysis. *Psychometrika* 40(1):33-51.

Gunz, P. and K. Harvati
2007 The Neanderthal "Chignon": Variation, Integration, and Homology. *Journal of Human Evolution* 52(3):262-274.

Harrington, Mark R.
1920 *Certain Caddo Sites in Arkansas*. Indian Notes and Monographs, Miscellaneous Series No. 10. Museum of the American Indian, Heye Foundation, New York.

Ioviţă, Radu
2009 Ontogenetic Scaling and Lithic Systematics: Method and Application. *Journal of Archaeological Science* 36(7):1447-1457.
2010 Comparing Stone Tool Resharpening Trajectories with the Aid of Elliptical Fourier Analysis. In *New Perspectives on Old Stones: Analytical Approaches to Paleolithic Technologies*, edited by S. J. Lycett and P. Chauhan, pp. 235-25310.1007/978-1-4419-6861-6_10. Springer-Verlag New York, New York.
2011 Shape Variation in Aterian Tanged Tools and the Origins of Projectile Technology: A Morphometric Perspective on Stone Tool Function. *PLoS One* 6(12):e29029.

Ioviţă, Radu and Shannon P. McPherron
2011 The Handaxe Reloaded: A Morphometric Reassessment of Acheulian and Middle Paleolithic Handaxes. *Journal of Human Evolution* 61(1):61-74.

Jensen, Richard J.
2003 The Conundrum of Morphometrics. *Taxon* 52:663-671.

Jolliffee, Ian T.
2002 *Principal Component Analysis*. Springer, New York.

Kendall, David G.
1981 The Statistics of Shape. In *Interpreting Multivariate Data*, edited by V. Barnett, pp. 75-80. Wiley, New York.
1984 Shape Manifolds, Procrustean Metrics, and Complex Projective Spaces. *Bulletin of the London Mathematical Society* 16(2):81-121.

Klingenberg, C. P.
2013 Visualizations in Geometric Morphometrics: How to Read and How to Make Graphs Showing Shape Changes. *Hystrix* 24:15-24.

Lenardi, Michael J. and Daria E. Merwin
2010 Towards Automating Artifact Analysis: A Study Showing Potential Applications of Computer Vision and Morphometrics to Artifact Typology. In *Morphometrics for Nonmorphometricians*, edited by A. M. T. Elewa, pp. 289-306. Lecture Notes in Earth Sciences10.1007/978-3-540-95853-6_13. Springer, New York.

Loponte, Daniel, Mercedes Okumura and Mirian Carbonera
2015 New Records of Fishtail Projectile Points from Brazil and its Implications for its Peopling. *Journal of Lithic Studies* 3(1).

Lycett, Stephen J.
2009 Quantifying Transitions: Morphometric Approaches to Palaeolithic Variability and Technological Change. In *Sourcebook of Paleolithic Transitions*, edited by M. Camps and P. Chauhan, pp. 79-9210.1007/978-0-387-76487-0_5. Springer.

Lycett, Stephen J., Noreen von Cramon-Taubadel and John A. J. Gowlett
2010 A Comparative 3D Geometric Morphometric Analysis of Victoria West Cores: Implications for the Origins of Levallois Technology. *Journal of Archaeological Science* 37(5):1110-1117.

Lycett, Stephen J. and Noreen von Cramon-Taubadel
2013 A 3D Morphometric Analysis of Surface Geometry in Levallois Cores: Patterns of Stability and Variability across Regions and their Implications. *Journal of Archaeological Science* 40(3):1508-1517.

Lycett, Stephen J., Noreen von Cramon-Taubadel and Metin I. Eren
2016 Levallois: Potential Implications for Learning and Cultural Transmission Capacities. *Lithic Technology* 41 (1): 19-38.

Lycett, Stephen J., Noreen von Cramon-Taubadel and Robert A. Foley
2006 A Crossbeam Co-ordinate Caliper for the Morphometric Analysis of Lithic Nuclei: A Description, Test and Empirical Examples of Application. *Journal of Archaeological Science* 33(6):847-861.

MacLeod, Norman
2017 Morphometrics, History, Development Methods and Prospects. *Zoological Systematics* 42(1):4-33.

Marcus, Leslie F., Marco Corti, Anna Loy, Gavin J. P. Naylor and Dennis E. Slice
1996 *Advances in Morphometrics* 10.1007/978-1-4757-9083-2. Springer, New York.

McKinnon, Duncan P.
2011 Foster Trailed-Incised: A GIS-Based Analysis of Caddo Ceramic Distribution. *Caddo Archaeology Journal* 21:71-88.

Mitteroecker, Philipp and Philipp Gunz
2009 Advances in Geometric Morphometrics. *Evolutionary Biology* 36(2):235-247.

Okumura, Mercedes and Astolfo G. M. Araujo
2013 Pontas Bifaciais no Brasil Meridional: Caracterização Estatística das Formas e suas Implicações Culturais. *Revista do Museu de Arqueologia e Etnologia, São Paulo,* 23(23):111-127.
2014 Long-Term Cultural Stability in Hunter–Gatherers: A Case Study using Traditional and Geometric Morphometric Analysis of Lithic Stemmed Bifacial Points from Southern Brazil. *Journal of Archaeological Science* 45:59-71.
2017 Fronteiras Sul e Sudeste: Uma Análise Morfométrica de Pontas Bifaciais de Minas Gerais, São Paulo, Paraná e Rio Grande do Sul (Brasil). *Journal of Lithic Studies* 4(1).
2018 Archaeology, Biology, and Borrowing: A Critical Examination of Geometric Morphometrics in Archaeology. *Journal of Archaeological Science* https://www.sciencedirect.com/science/article/pii/S0305440317301462?via%3Dihub.

Perttula, Timothy K.
2010 Woodland and Caddo Ceramic Traditions in East Texas. In *Regional Summaries of Prehistoric and Early Historic Ceramics in Texas for the Council of Texas Archeologists*, edited by L. W. Ellis and T. K. Perttula, pp. 13-41. Council of Texas Archeologists, Austin.

2015 Diversity in Ancestral Caddo Vessel Forms in East Texas Archaeological Sites. *Journal of Northeast Texas Archaeology* 56:1-19.

Picin, Andrea, Manuel Vaquero, Gerd-Christian Weniger and Eudald Carbonell
2014 Flake Morphologies and Patterns of Core Configuration at the Abric Romaní Rock-Shelter: A Geometric Morphometric Approach. *Quaternary International* 350:84-93.

R Development Core Team
2018 R: A Language and Environment for Statistical Computing. R Foundation for Statistical Computing, Vienna, Austria.

Rezek, Zeljko, Sam Lin, Radu Iovita and Harold L. Dibble
2011 The Relative Effects of Core Surface Morphology on Flake Shape and Other Attributes. *Journal of Archaeological Science* 38(6):1346-1359.

Rice, Prudence M.
1991 Specialization, Standardization, and Diversity: A Retrospective. In *The Ceramic Legacy of Anna O. Shepard*, edited by R. L. Bishop and F. W. Lange, pp. 257-279. University of Colorado Press, Niwot.

Richtsmeier, Joan T., James M. Cheverud and Subhash Lele
1992 Advances in Anthropological Morphometrics. *Annual Review of Anthropology* 21(1):283-305.

Rivero, Diego and Guillermo Heider
2017 Geometric Morphometrics in Lanceolate Projectile Points from Central Hills, Argentina. *Revista del Museo de Antropología* 1:75-82.

Rohlf, F. James
1990 Morphometrics. *Annual Review of Ecology and Systematics* 21(1):299-316.
1999 Shape Statistics: Procrustes Superimpositions and Tangent Spaces. *Journal of Classification* 16(2):197-223.

Rohlf, F. James and Marco Corti
2000 Use of Two-Block Partial Least-Squares to Study Covariation in Shape. *Systematic Biology* 49(4):740-753.

Rohlf, F. James and Leslie F. Marcus
1993 A Revolution in Morphometrics. *Trends in Ecology & Evolution* 8(4):129-132.

Rohlf, F. James and Dennis Slice
1990 Extensions of the Procrustes Method for the Optimal Superimposition of Landmarks. *Systematic Zoology* 39(1):40-59.

Ros, Jérôme, Allowen Evin, Laurent Bouby and Marie-Pierre Ruas
2014 Geometric Morphometric Analysis of Grain Shape and the Identification of Two-Rowed Barley (Hordeum vulgare subsp. distichum L.) in Southern France. *Journal of Archaeological Science* 41:568-575.

Selden Jr., Robert Z.
2017 Asymmetry of Caddo Ceramics from the Washington Square Mound Site: An Exploratory Analysis. *Digital Applications in Archaeology and Cultural Heritage* 5:21-28.
2018a Ceramic Morphological Organisation in the Southern Caddo Area: The Clarence H. Webb Collections. *Journal of Cultural Heritage* (revised and resubmitted).
2018b Ceramic Morphological Organization: Quiddity of Shape for Hickory Engraved Bottles. vol. 2018. Stephen F. Austin State University, Nacogdoches.

Selden Jr., Robert Z., Timothy K. Perttula and Michael J. O'Brien
2014 Advances in Documentation, Digital Curation, Virtual Exhibition, and a Test of 3D Geometric Morphometrics: A Case Study of the Vanderpool Vessels from the Ancestral Caddo Territory. *Advances in Archaeological Practice* 2(2):1-15.

Serwatka, Kamil
2015 Shape Variation of Middle Palaeolithic Bifacial Tools from Southern Poland: A Geometric Morphometric Approach to Keilmessergruppen Handaxes and Backed Knives. *Lithics* 35:18-32.

Serwatka, Kamil and Felix Riede
2016 2D Geometric Morphometric Analysis Casts Doubt on the Validity of Large Tanged Points as Cultural Markers in the European Final Palaeolithic. *Journal of Archaeological Science: Reports* 9:150-159.

Sherratt, E., D. J. Gower, C. P. Klingenberg and M. Wilkinson
2014 Evolution of Cranial Shape in Caecilians (Amphibia: Gymnophiona). *Evolutionary Biology* 41:528-545.

Sholts, Sabrina B., Dennis J. Stanford, Louise M. Flores and Sebastian K. T. S. Wärmländer
2012 Flake Scar Patterns of Clovis Points Analyzed with a New Digital Morphometrics Approach: Evidence for Direct Transmission of Technological Knowledge across Early North America. *Journal of Archaeological Science* 39(9):3018-3026.

Shott, Michael J.
2011 History Written in Stone: Evolutionary Analysis of Stone Tools in Archeology. *Evolution: Education and Outreach* 4(3):435-445.

Shott, Michael J. and Brian W. Trail
2010 Exploring New Approaches to Lithic Analysis: Laser Scanning and Geometric Morphometrics. *Lithic Technology* 35(2):195-220.

Slice, Dennis E.
2001 Landmark Coordinates Aligned by Procrustes Analysis Do Not Lie in Kendall's Shape Space. *Systematic Biology* 50(1):141-149.

2007 Geometric Morphometrics. *Annual Review of Anthropology* 36(1):261-281.

Smith, Heather L.
2010 A Behavioral Analysis of Clovis Point Morphology using Geometric Morphometrics, Department of Anthropology, Texas A&M University.

Smith, Heather L. and Thomas J. DeWitt
2016 The Northern Fluted Point Complex: Technological and Morphological Evidence of Adaptation and Risk in the Late Pleistocene-Early Holocene Arctic. *Archaeological and Anthropological Sciences* 9(8):1799-1823.

Smith, Heather L. and Ted Goebel
2018 Origins and Spread of Fluted-Point Technology in the Canadian Ice-Free Corridor and Eastern Beringia. *Proceedings of the National Academy of Sciences* 10.1073/pnas.1800312115.

Smith, Heather L., Ashley M. Smallwood and Thomas J. DeWitt
2014 A Geometric Morphometric Exploration of Clovis Fluted-Point Shape Variability. In *Clovis: On the Edge of a New Understanding*, edited by A. M. Smallwood and T. A. Jennings, pp. 161-180. Texas A&M University Press, College Station.

Suhm, Dee Ann and Edward B. Jelks
1962 *Handbook of Texas Archeology: Type Descriptions*. Texas Archeological Society, Austin.

Suhm, Dee Ann, Alex D. Krieger and Edward B. Jelks
1954 An Introductory Handbook of Texas Archeology. *Bulletin of the Texas Archeological Society* 25:1-562.

Swanton, John R.
1942 *Source Material on the History and Ethnology of the Caddo Indians*. Bulletin 132. Bureau of American Ethnology. Smithsonian Institution, Washington.

Thulman, David K.
2012 Discriminating Paleoindian Point Types from Florida using Landmark Geometric Morphometrics. *Journal of Archaeological Science* 39(5):1599-1607.

Topi, John R., Christine S. VanPool, Kyle D. Waller and Todd L. VanPool
2017 The Economy of Specialized Ceramic Craft Production in the Casas Grandes Region. *Latin American Antiquity* 29(1):122-142.

Velhagen, William A. and V. Louise Roth
1997 Scaling of the Mandible in Squirrels. *Journal of Morphology* 232(2):107-132.

Wang, Wei, Stephen J. Lycett, Noreen von Cramon-Taubadel, Jennie J. H. Jin and Christopher J. Bae
2012 Comparison of Handaxes from Bose Basin (China) and the Western Acheulean Indicates Convergence of Form, not Cognitive Differences. *PLoS One* 7(4):e35804.

Webb, Clarence H.
1959 *The Belcher Mound, A Stratified Caddoan Site in Caddo Parish, Louisiana* Memoirs No. 16. Society for American Archaeology, Salt Lake City.

1963 The Smithport Landing Site: An Alto Focus Component in DeSoto Parish, Louisiana. *Bulletin of the Texas Archeological Society* 32:143-187.

Wilczek, J., F. Monna, P. Barral, L. Burlet, C. Chateau and N. Navarro
2014 Morphometrics of Second Iron Age ceramics – strengths, weaknesses, and comparison with traditional typology. *Journal of Archaeological Science* 50:39-50.

Wilczek, J., F. Monna, M. Gabillot, N. Navarro, L. Rusch and C. Chateau
2015 Unsupervised Model-Based Clustering for Typological Classification of Middle Bronze Age Flanged Axes. *Journal of Archaeological Science: Reports* 3:381-391.